Biomaterials 87 (2016) 1–17

Contents lists available at ScienceDirect

Biomaterials

journal homepage: www.elsevier.com/locate/biomaterials

Simple and versatile synthetic polydopamine-based surface supports reprogramming of human somatic cells and long-term self-renewal of human pluripotent stem cells under defined conditions

Ping Zhou [a, b], Fujian Wu [d], Tiancheng Zhou [c], Xiujuan Cai [c], Siqi Zhang [b], Xiaohong Zhang [b], Qiuhong Li [b, c], Yongliang Li [a], Yunfei Zheng [a], Mengke Wang [a], Feng Lan [d], Guangjin Pan [c, **], Duanqing Pei [c], Shicheng Wei [a, b, *]

[a] Department of Oral and Maxillofacial Surgery, Laboratory of Interdisciplinary Studies, School and Hospital of Stomatology, Peking University, Beijing, 100081, China
[b] Center for Biomedical Materials and Tissue Engineering, Academy for Advanced Interdisciplinary Studies, Peking University, Beijing, 100871, China
[c] Key Laboratory of Regenerative Biology, Guangzhou Institutes of Biomedicine and Health, Chinese Academy of Sciences, Guangzhou, 510530, China
[d] Beijing Institute of Heart Lung and Blood Vessel Diseases, Beijing Anzhen Hospital, Capital Medical University, Beijing, 100029, China

ARTICLE INFO

Article history:
Received 30 January 2016
Accepted 4 February 2016
Available online 10 February 2016

Keywords:
Polydopmine
Carboxymethyl chitosan
Peptide
Human embryonic stem cells
Human induced pluripotent stem cells
Chemically-defined

ABSTRACT

Human pluripotent stem cells (hPSCs) possess great value in the aspect of cellular therapies due to its self-renewal and potential to differentiate into all somatic cell types. A few defined synthetic surfaces such as polymers and adhesive biological materials conjugated substrata were established for the self-renewal of hPSCs. However, none of them was effective in the generation of human induced pluripotent stem cells (hiPSCs) and long-term maintenance of multiple hPSCs, and most of them required complicated manufacturing processes. Polydopamine has good biocompatibility, is able to form a stable film on nearly all solid substrates surface, and can immobilize adhesive biomolecules. In this manuscript, a polydopamine-mediated surface was developed, which not only supported the reprogramming of human somatic cells into hiPSCs under defined conditions, but also sustained the growth of hiPSCs on diverse substrates. Moreover, the proliferation and pluripotency of hPSCs cultured on the surface were comparable to Matrigel for more than 20 passages. Besides, hPSCs were able to differentiate to cardiomyocytes and neural cells on the surface. This polydopamine-based synthetic surface represents a chemically-defined surface extensively applicable both for fundamental research and cell therapies of hPSCs.

1. Introduction

Human pluripotent stem cells (hPSCs), including human embryonic stem cells (hESCs) and human induced pluripotent stem cells (hiPSCs), have been studied as a potential cell source to treat a host of diseases, since they have the unique ability of self-renewal and the potential to differentiate into any specialized human cells [1,2]. Considerable progress has been made in the development of culture systems for derivation, self-renewal and differentiation of hPSCs [3]. Generally, hPSCs are cultured on feeder cell layers of human and other species (including their extracts) [4–8] or Matrigel [9]. However, preparing feeder cells takes too much time and cannot produce hPSCs in large scale [10]. In addition, chemically undefined Matrigel generally has some problems such as immunogenicity, animal pathogens, and variability between batches [11–13]. Native and recombinant predominant adhesive proteins in Matrigel [13–19], protein fragments [20–22] and recombinant spider silk [16,23] have been explored for the chemically defined culture of hPSCs from cellular therapies. Nevertheless, besides considerable expense, the batch-to-batch variability of these biological materials results in very limited applications [24]. In this regard, a few synthetic surfaces have been developed for the self-renewal of hPSCs [24–32], because they are much more economical and stable in comparison to the above

* Corresponding author. Department of Oral and Maxillofacial Surgery, Laboratory of Interdisciplinary Studies, School and Hospital of Stomatology, Peking University, Beijing, 100081, China.
** Corresponding author.
E-mail addresses: pan_guangjin@gibh.ac.cn (G. Pan), sc-wei@pku.edu.cn (S. Wei).

http://dx.doi.org/10.1016/j.biomaterials.2016.02.012
0142-9612/

mentioned biological materials. Unfortunately, these synthetic surfaces have their own drawbacks and limitations in fundamental research and clinical application of hPSCs. First, none of them has been reported to support the reprogramming of multiple human somatic cells into hiPSCs. Second, most of these synthetic surfaces do not present effectiveness for the long-term self-renewal of multiple hPSCs [24]. Third, their preparation processes such as UV-ozone activation [25–28] and surface initiated polymerization (SIP) [24,30] not only use biologically inert or toxic materials, but also require very complicated procedures, which cannot meet the criteria of Good Manufacturing Practices (GMP) protocols. At last, some surfaces such as hydrogels [27], nanofibers [29] and membranes [32] need extra incubation with culture medium. A simple, scalable and effective synthetic surface that can support the reprogramming, long-term self-renewal and differentiation of hPSCs under chemically defined conditions is highly desirable and critical for the successful application of hPSCs.

Polydopamine (PDA), inspired by the composition of adhesive proteins in mussels, has been used as a universal surface modification agent for the immobilization of biomolecules onto a wide variety of substrates for years [33,34]. A strongly attached PDA film will be formed on the surfaces by simply immersing any solid substrates into dopamine solution under slightly alkaline condition (pH = 8.5). Combined with biomolecules that support the adhesion and self-renewal of hPSCs, PDA-mediated surface modification possesses good prospect to be an easy-handle process that allows hPSCs to be cultured on diverse solid substrates. A synthetic peptide derived from vitronectin (VN peptide) with effectiveness for survival of hPSCs was chosen to be grafted on PDA coating for the following reasons: (a) it is much cheaper to manufacture than proteins and their fragments, (b) synthetic peptides exhibit nearly no concerns regarding immunogenicity, (c) hPSCs could survive on peptide-conjugated surface without additional culture medium incubation step [26,35]. However, PDA film possess strong binding ability with thiol, amine and imidazole groups [36], which could affect orientation and three-dimensional structure of biomolecules that contain these groups, and result in reduced even abolished bioactivity. Surface characterization proved that VN peptide was grafted on the PDA-decorated cell culture surface, but this surface could not support the adhesion of hPSCs. This is why PDA coating have rarely been utilized for the generation and self-renewal of hPSCs, although many studies have confirmed its effectiveness in the fields such as tissue engineering [37–43], drug carriers [44,45] and biosensor [46,47].

Great effort has been made to conjugate biomolecules onto PDA decorated surface for the survival of hPSCs. Synthetic surfaces that presenting carboxyl group had been widely applied to conjugate peptides or polymers for the self-renewal of hPSCs [24,26,28,30,35]. In this manuscript, carboxymethyl chitosan (CMC), a derivative of chitosan, was used as a linker to orthogonally and controllably attach VN peptide to the synthetic PDA-surface for the culture of hPSCs. CMC not only has good biocompatibility, biodegradability and bioactivity [48,49], but also contains both amine and carboxyl group. This newly-developed surface is able to support the reprogramming of human somatic cells into hiPSCs, long-term self-renewal of four hPSCs lines and differentiation of hPSCs into neural cells and cardiomyocytes under defined conditions. We believe our scalable, controllable and sustainable polydopamine-based modification method will be useful for fundamental research and clinical application of hPSCs.

2. Materials and methods

2.1. Polydopamine-mediated surface modification

For PDA coating, 5 ml of 2 g L^{-1} dopamine solution (10 mM Tris–HCl buffer, pH = 8.5) was added into each well of 6-well cell culture plates (Corning, USA) and gently shaken at 37 °C for overnight. The PDA-coated plates were ultrasonically cleaned in sterile distilled water for 5 min to remove the physically adsorbed PDA particles. They were then immersed in 5 ml of freshly prepared 10 mg ml^{-1} L-lysine or 3% (w/v) CMC solution (distilled water buffer) with shaking for 24 h at 37 °C. The PDA-Lys/CMC coated surfaces were thoroughly washed with sterile distilled water and allowed to be dried. Those processes were conducted in a biological safety cabinet (MSC-Advantage 1.2, Thermo, Germany), and all reaction solution had been sterilized by 0.22 μm filter (Millipore, USA) before use.

2.2. Immobilization of VN peptide

PDA-modified 6-well plates were prepared as previously mentioned, 1 ml of 1 mM VN peptide in sterile DPBS buffer (PBS solution without Ca^{2+} and Mg^{2+}, pH = 7.4) was then added into each well at 4 °C for overnight to prepare PDA-VN surface. Moreover, PDA-Lys-VN and PDA-CMC-VN coated plates were manufactured as follows: 3 ml of activation solution containing 2 mM EDC and 5 mM NHS (0.1 M MES buffer, pH = 5.6, filtered by 0.22 μm filter) was poured into each well of PDA-Lys/CMC modified plates for 40 min at RT; After rinsing with sterile DPBS buffer, 1 ml of 1 mM VN peptide was pipetted to each activated well and incubated at 4 °C for overnight. These peptide-conjugated plates were washed with sterile DPBS buffer to remove the unattached peptide. All those processes were conducted in a biological safety cabinet. Moreover, the content of VN peptide immobilized on diverse surfaces of PDA-VN, PDA-Lys-VN and PDA-CMC-VN were visualized using FITC-labeled VN peptide (FITC-Ac-KGGPQVTRGDVFTMP).

2.3. Culture of hESCs and hiPSCs

The hESCs lines H1 (P46) and H9 (P46) were provided by WiCell Research Institute (Madison, Wisconsin) [8]. The hiPSCs lines hNF-C1 (P35) and UMC-C1 (P42) that derived via sendai virus (Invitrogen, USA) were supplied by Guangzhou Institutes of Biomedicine and Health (Guangzhou, China) as gifts. The hNF-C1 hiPSCs was generated from human skin fibroblasts, and the UMC-C1 hiPSCs was derived from human umbilical cord blood cells (hUMC). These hESCs and hiPSCs were cultured on Matrigel (BD Biosciences, Canada) coated plates under standard cell culture conditions (37 °C, 100% humidity and 5% CO_2) in an incubator (HERAcell 150i, Thermo, USA). Matrigel was diluted with Dulbecco's modified eagle medium/F12 (DMEM/F12; Gibco, USA) at a ratio of 1:80 on ice. Cells were fed daily and passaged at 1:3 splitting ratio every 3–4 days by exposure to 0.5 mM EDTA (Aladdin, China) for 4–5 min at 37 °C. In this manuscript, hPSCs were cultured in chemically defined mTeSR1 medium (Stem Cell Technologies, Canada) unless otherwise specified.

2.4. Survival of hESCs and hiPSCs on various polydopamine-based surfaces

H1 hESCs and hNF-C1 hiPSCs were, respectively, seeded on PDA-VN, PDA-Lys-VN and PDA-CMC-VN decorated 6-well plates at a density of 23,500 cells·cm^{-2} as single cells using 0.25% Trypsin/EDTA for 2–3 min (Stem Cell Technologies, Canada), and Matrigel was used as a control. The medium was changed every day and the cell attachment was measured after 4 day of culturing using the cell counting kit-8 assay (CCK-8, Dojindo, Japan) according to manufacturer's instructions. Three parallel wells were used for each group.

2.5. Cell attachment on the PDA-CMC-VN surface

H1 hESCs and hNF-C1 hiPSCs were applied to investigate the effect of VN peptide concentration, dissociation methods and ROCK inhibitor (Y-27632, Sigma–Aldrich, USA) on the adhesion and survival of hPSCs in mTeSR1 medium. A dilution series of VN peptide solutions (0.25 mM, 0.5 mM, 0.75 mM and 1 mM) with a volume of 1 ml were, respectively, injected into each activated PDA-CMC modified well of 6-well plates overnight at 4 °C. After rinsing with DMEM/F12 (Hyclone, USA) three times, H1 hESCs and hNF-C1 hiPSCs were seeded on those surfaces at a density of 23,500 cells·cm^{-2} as single cells using 0.25% Trypsin/EDTA. In parallel, single cells were seeded on 6-well plates coated with Matrigel at the same density. Then, PDA-CMC modified 6-well plates were reacted with 1 mM VN peptide as previously mentioned. H1 hESCs and hNF-C1 hiPSCs were digested as colonies by exposure to 0.5 mM EDTA (Sigma–Aldrich, USA) for 4–5 min at 37 °C, and single cells were acquired using 0.25% Trypsin/EDTA. After cell counting, H1 hESCs and hNF-C1 hiPSCs were seeded on PDA-CMC-VN surface at a density of 23,500 cells·cm^{-2} in four different conditions (single cells without Y-27632, single cells with Y-27632, colonies without Y-27632 and colonies with Y-27632), and Matrigel-coated plates was conducted as controls. Besides, after cultured in E8 medium (Cellapybio, China) on Matrigel surface for several passages, H1 hESCs and hNF-C1 hiPSCs were seeded on PDA-CMC-VN and Matrigel surface in E8 as colonies at a density of 23,500 cells·cm^{-2}. 5 μM Y-27632 was supplemented for a day and cells were fed daily. The numbers of survive cells were measured after 4 day of culture using the CCK-8 reagent. Each group included 3 wells, and every test was performed in triplicate.

2.6. hiPSCs cultured on diverse substrates decorated by PDA-CMC-VN

Glass, PDMS and Ti were ultrasonically cleaned in acetone, absolute ethyl alcohol and distilled water for 20 min respectively, and then dried under a stream of nitrogen. Each side of substrates (glass, PDMS and Ti) was sterilized under UV irradiation for 30 min and placed in 6-well plates. They were then sequentially modified by PDA/CMC/VN peptide as previously mentioned. hNF-C1 hiPSCs were seeded on those modified substrate surfaces as colonies with the supplementation of Y-27632 at a density of 23,500 cells·cm^{-2}. After 4 day of culture, cells on those substrates were observed using a phase contrast microscope (CKX31SF, Olympus, Japan) or upright metallurgical microscope (BX51M, Olympus, Japan). Moreover, the Oct-4 expression of those cells was evaluated using flow cytometry.

2.7. Characterization

The alteration of chemical composition and morphology for various substrates (PS, glass, PDMS and Ti) before and after PDA/CMC/VN modifications were analyzed by X-ray photoelectron spectroscopy (XPS), water contact angle and atomic force microscopy (AFM). The chemical constituents were characterized by XPS (Kratos Analytical Ltd, UK) at 15 kV and 10 mA. The surface hydrophilicity was detected by contact angle goniometry (Dataphysics Instrument, Germany). Six measurements were performed for each surface at ambient temperature based on the sessile drop method, and the mean value was taken as the reported result. In addition, the surface topography was detected by AFM (Dimension ICON, Bruker, USA) using ScanAsyst automatic image optimization technology with 1.0 Hz scan rates. Ra and Z were applied to evaluate the surface roughness on the basis of scan areas (1 μm × 1 μm and 5 μm × 5 μm). Moreover, the surface morphology and relative Young's modulus of PS that was sequentially modified by PDA/CMC/VN peptide in PBS buffer were evaluated using Bruker MultiMode 8 scanning probe microscope (Veeco, USA).

2.8. RNA extraction and sequencing

H1 hESCs and hNF-C1 hiPSCs on Matrigel were seeded as colonies on PDA-CMC-VN and Matrigel surface in mTeSR1 medium for 24 h before harvest. Total RNA was extracted using the RNeasy Mini Kit and DNase1 digestion kit (Qiagen, Germany). RNA quality was assessed using the ND-2000 Nanodrop to ensure an A260:A280 ratio of 1.9–2.0 and A260:A230 ratio above 2.2. Sequencing libraries were constructed with TruSeq RNA sample prep kit (Illumina, USA) according to the manufacturer's manual. Sequencing was performed using Illumina Hiseq™ 2000 device (Illumina, USA). The quality controlled RNA-seq reads were mapped to the corresponding human genome assembly hg19 using bowtie (v1.0.1). The expression abundance was measured by transcripts per million (TPM) and calculated with RSEM (v1.2.12).

2.9. Derivation of hiPSCs on PDA-CMC-VN surface

The generation of hiPSCs from both 2 donors of human urine derived cells (hUC) and human umbilical cord blood cells (hUMC) was conducted in Guangzhou Institutes of Biomedicine and Health (Guangzhou, China), and the episomal plasmids and methods have been reported previously [50]. Briefly, oriP/EBNA episomal vectors carrying a combination of reprogramming factors encoded by Oct-4 (POU5F1), Sox-2, SV40LT, Klf-4 and microRNA cluster MIR302–367 were applied for the reprogramming. Three million cells, both for hUC and hUMC, were transfected with oriP/EBNA episomal vectors by electroporation apparatus (Amaxa Nucleofector II, Lonza, Switzerland) according to the manufacturer's instructions. Then, half a million cells were placed into each well of PDA-CMC-VN coated 6-well cell culture plates. The transfected cells were cultured in E7 medium with the supplementation of sodium butyrate. The cells were fed every other day and the medium was changed to mTeSR1 when ESC-like hiPSC colonies appeared. When reprogramming for about 3 weeks, hiPSCs were picked onto Matrigel surface in mTeSR1. These acquired hiPSCs were analyzed using assays such as flow cytometry, immunostaining, karyotyping, embryoid body (EB) and teratoma formation.

2.10. Long-term culture of hESCs and hiPSCs on PDA-CMC-VN surface

The long-term self-renewal of hPSCs was performed on PDA-CMC-VN modified 6-well plates. hESCs (H1 and H9) and hiPSCs (hNF-C1 and UMC-C1) on Matrigel were harvested by 0.5 mM EDTA treatment for 4–5 min at 37 °C. Cells were then dissociated by pipetting and seeded on PDA-CMC-VN surface at a splitting ratio of 1:3 in mTeSR1 medium containing 5 μM Y-27632. ROCK inhibitor Y-27632 was only added while passaging and the medium was changed freshly every day. The morphology of cells was observed every day using an inverted microscope (CKX41, Olympus, Japan). Differentiated cells were marked and removed mechanically by a negative pressure aspirator (YX932D, Baojia, China). Depending on size and density of colonies, cells were passaged every 3–5 days at a splitting ratio of 1:3 by treatment with EDTA and transferred onto new PDA-CMC-VN surface. Besides, we serially passaged H1 hESCs on PDA-CMC-VN surface in E8 for 10 passages under the same conditions in mTeSR1. The cells at various passages were also maintained in frozen stock solution containing 90% mTeSR1 medium and 10% DMSO (Amresco, USA), and stored in liquid nitrogen for future usage.

a

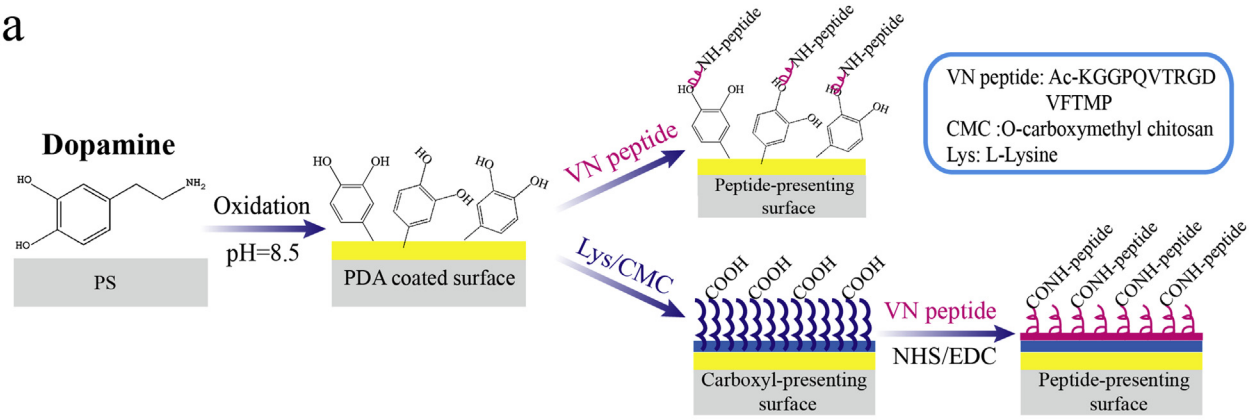

b

	PDA-VN	PDA-Lys-VN	PDA-CMC-VN
VN concentration ($\mu g \cdot cm^{-2}$)	67.74±17.27	51.70±13.74	48.72±14.52
Contact angle (degree)	55.13±5.94	28.23±6.38	30.88±3.52
H1 adhesion (% of Matrigel)	0	0	2.44±0.43
hNF-C1 adhesion (% of Matrigel)	0	0	9.67±1.93
Passages	0	0	>20

c

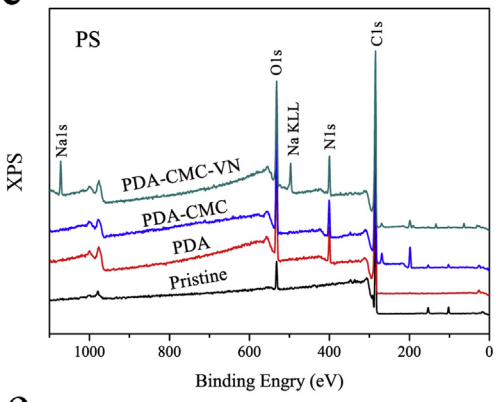

d

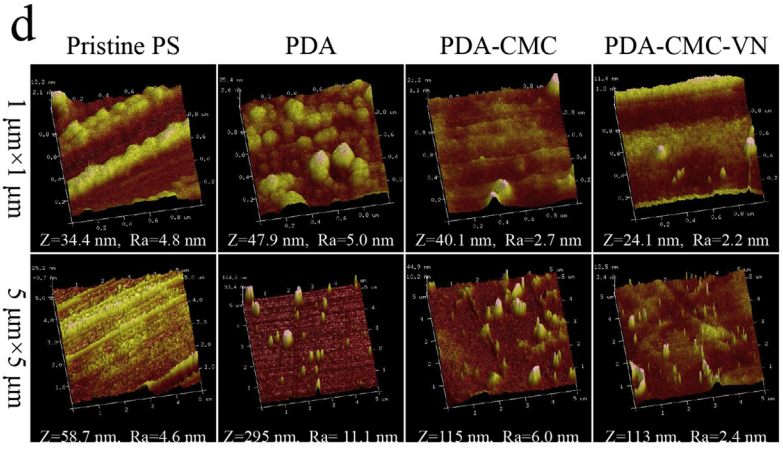

e

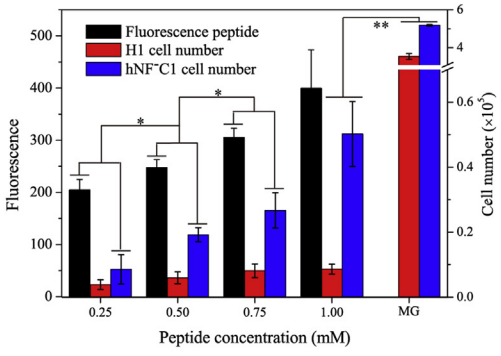

f

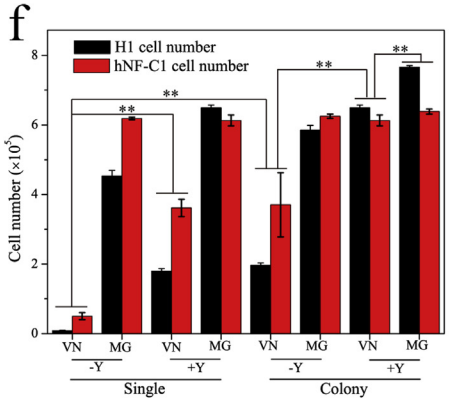

g

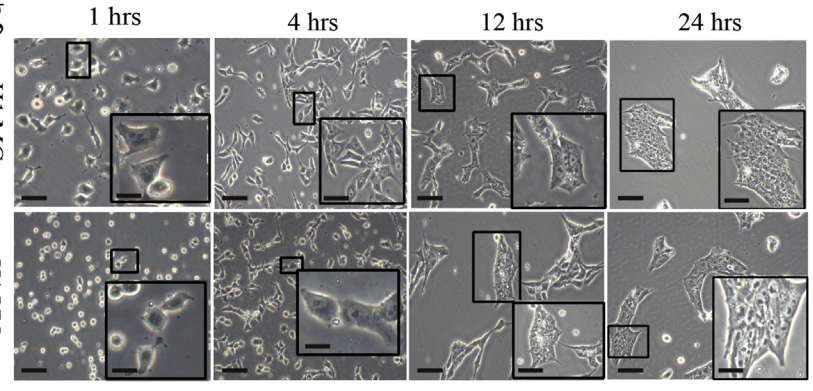

Fig. 1. Development of the PDA-mediated peptide-conjugated surface. (a) Schematic representation of the coating processes for PDA-VN, PDA-Lys-VN and PDA-CMC-VN surface. (b) Table lists VN concentration, contact angle, cell adhesions of H1 hESCs and hNF-C1 hiPSCs after seeded 237,500 cells as single cells for 4 days (% of Matrigel, mean ± sd) and number of passages achieved on PDA-VN, PDA-Lys-VN and PDA-CMC-VN decorated 6-well culture plates. (c) XPS wide spectra of unmodified PS and sequentially decorated by PDA/CMC/VN

2.11. Cell population-doubling time

The cell doubling times of H1 hESCs and hNF-C1 hiPSCs on PDA-CMC-VN and Matrigel surface were analyzed as time required for the area of a colony to increase two-fold, and estimated as an exponential function [25,51]. Briefly, the colony area was calculated using the surface area equation of an ellipse ($\pi \times a \times b/4$, where a and b are the horizontal and longitudinal diameters), and the diameters was measured using ImageJ software. Three areas containing colonies were marked for H1 hESCs and hNF-C1 hiPSCs on surfaces of PDA-CMC-VN and Matrigel in ten passages and photographed every 24 h by a phase contrast microscope (CKX31SF, Olympus, Japan) with CCD camera (MP3.3-RTV, Olympus, Japan).

2.12. Expression of pluripotency markers

As provided in the Supporting Information, for hPSCs cultured on PDA-CMC-VN and Matrigel surface, the pluripotency markers expression of genes (Oct-4, Nanog, Sox-2 and Rex-1) was measured by reverse-transcription PCR (RT-PCR), and the expression of proteins (Oct-4, SSEA-3 and Tra-1 60) was investigated using fluorescence activating cell sorter (FACS) and immunofluorescence.

2.13. Karyotyping

hPSCs that cultured on PDA-CMC-VN surface were passaged onto Matrigel for karyotyping analysis. The samples were submitted for karyotyping analysis by standard G banding technique (Cell inspore Biotechnology Co., Ltd, China). A minimum of 20 metaphase spreads were analyzed, and an additional 20 were counted. The final karyotype was stated if it was present in more than 85% of them.

2.14. Cell extracts preparation and detection of telomerase activity

The telomerase activities of H1 hESCs and hNF-C1 hiPSCs after 20 passages on PDA-CMC-VN and Matrigel surface were measured using a novel method based on quartz crystal microbalance (QCM) that we previously reported [52], and those of H1 hESCs and hNF-C1 hiPSCs at P0 on Matrigel surface were conducted as controls.

2.15. Embryoid body formation

hPSCs were incubated with 1 mg ml^{-1} Dispase (Invitrogen, USA) for 5–7 min when grown to 80% confluence on both PDA-CMC-VN and Matrigel surface. Then, cells were rinsed with DMEM/F12 three times and mechanically scraped from the plates in knockout DMEM/F12 medium (GIBCO, USA) supplemented with 20% fetal bovine serum (FBS; GIBCO, USA), 2 mM L-glutaMax (GIBCO, USA), 1% (wt/vol) non-essential amino acids (GIBCO, USA), 0.1 mM 2-β-mercaptoethanol (GIBCO, USA). After 8 days in suspension on low adherence plates (Corning, USA), the embryoid bodies were transferred into 0.1% gelatin (Sigma–Aldrich, USA) coated 6-well plates in the same medium for another 8 days before cell total RNA was extracted. The medium for each condition was changed every other day. Primers used in this study were provided in Table S1 and β-actin was used for normalization.

2.16. Teratoma formation assays

hPSCs samples were harvested using Dispase at 0.5 mg ml^{-1} for 5 min and one million cells were injected into the flanks of nude mice subcutaneously. The mice were sacrificed when teratoma size reached 1 cm in diameter and the excised tumor tissues were fixated in 1% formalin for 24 h. After 70% ethanol treatment, the tumors were embedded in paraffin and processed into 4 mm thick sections. Then, sections were stained with hematoxilin/eosin (HE) and histologically analyzed.

2.17. In vitro differentiation of hPSCs on PDA-CMC-VN surface

A recently published process was applied for chemically defined generation of human cardiomyocytes from E8 medium cultured hNF-C1 hiPSCs on PDA-CMC-VN and Matrigel surface [53]. After inducing for 12 days, the differentiation towards cardiomyocytes was analyzed using RT-PCR, FACS and immunofluorescence staining. Primary antibodies such as mouse monoclonal IgG1 TNNT2 (ab8295, Abcam), rabbit monoclonal IgG α-ACTININ (H-300, Santa Cruz) and their corresponding secondary antibodies purchased from Life technologies were utilized for FACS and immunofluorescence staining. The primer sequences used for the RT-PCR were listed in Table S1.

Moreover, after 15 passages on PDA-CMC-VN surface, H9 hESCs were differentiated towards neural cells using the STEMdiff neural system (Stem Cell Technologies, Canada) according to the manufacturer's instructions, which was confirmed by immunofluorescence staining using primary antibodies such as SOX-1 (R&D AF3369, USA), Nestin (R&D MAB1259, USA), MAP-2 (Millpore AB5622, USA), Anti-β-Tubulin III (TUJ-1, Sigma–Aldrich T3952, USA) and their corresponding secondary antibodies that purchased from R&D or Life technologies.

2.18. Statistical analysis

All data were expressed as the average of at least three replicate experiments and were presented as the mean ± standard deviation. Student's t-test was used to determine the significant differences among the groups, and p values < 0.05 were considered statistically significant.

3. Results and discussion

3.1. Design of PDA-CMC-VN surface for survival of hPSCs

We developed a PDA-VN surface for the survival of hPSCs as shown in Fig. 1a. Surface characterization via XPS and water contact goniometry confirmed that PDA and VN peptide were grafted on the plate surfaces (shown in supporting results). Although high concentration of VN peptide (67.74 ± 17.27 ng cm^{-2}) was detected on PDA-VN surface, no survival of H1 hESCs or hNF-C1 hiPSCs was found, suggesting VN peptide grafted directly on PDA coating could not support the adhesion of hPSCs (Fig. 1b). This is consistent with a very recent report that PDA coated with VN-dimer, not VN peptide, allows self-renewal of hPSCs [31]. Unfortunately, only one hiPSCs and H9 hESCs were cultured on that surface for 10 passages.

peptide. (d) AFM surface topographies of those samples with scan area of 1 μm × 1 μm and 5 μm × 5 μm. Insert are values of Z range and Ra for surfaces of those samples. (e) Peptide concentration-dependent H1 hESCs and hNF-C1 hiPSCs attachment and growth. PDA-CMC-VN decorated 6-well plates were prepared with serial dilutions of VN or FITC-labeled VN peptide. 237,500 H1 hESCs and hNF-C1 hiPSCs were respectively seeded on each of PDA-CMC-VN and Matrigel surfaces as single cells and cultured for 4 days. (f) Distinct cell survival of H1 hESCs and hNF-C1 hiPSCs depending on dissociation methods and Y-27632. Data represent the cell numbers of live cells after seeded 237,500 cells as single cells (single) or colonies (colony) on PDA-CMC-VN and Matrigel surface with or without Y-27632 for 4 days. (g) Serial phase-contrast images of single H1 hESCs on PDA-CMC-VN and Matrigel surface in mTeSR1 medium at initial attachment (1 h, 4 h, 12 h and 24 h). Images at the bottom right show an enlarged view of enclosed boxes. Scale bars, 200 μm
*Represents $p < 0.05$ and ** Represents $p < 0.01$ ($n = 3$).

Moreover, the cell population-doubling time and the percentage of hPSCs that maintained pluripotency at each passage on the synthetic surface are not shown. At last, it did not provide any evidence of supporting the generation and differentiation of hPSCs.

In this study, PDA modified surface was conjugated with Lys and CMC, biomolecules containing groups of both amine and carboxyl, via reaction between amino groups and catechol/quinone groups through Michael addition and Schiff-base reactions [54], and then reacted with VN peptide using standard NHS/EDC chemistry. These surface modification processes were verified by XPS and contact angle goniometry (shown in supporting results). The concentration of VN peptide on PDA-Lys-VN (51.70 ± 13.74 ng cm^{-2}) and PDA-CMC-VN surface (48.72 ± 14.52 ng cm^{-2}) were both lower than that on PDA-VN surface (Fig. 1b). We had performed more than fifteen biological replicates to assay the adhesion of H1 hESCs and hNF-C1 hiPSCs on PDA-Lys-VN surface. In most cases, whether dissociated as single cells or colonies, none or few colonies of H1 hESCs and hNF-C1 hiPSCs were found on PDA-Lys-VN surface. These results suggested that PDA-Lys-VN surface was not suitable for the long-term proliferation of hPSCs. A number of biological replicates were also conducted to investigate the adhesion and survival of H1 hESCs and hNF-C1 hiPSCs on PDA-CMC-VN surface. Many survive hPSCs colonies were observed at each test, indicating that PDA-CMC-VN surface is much better than PDA-Lys-VN surface for the culture of hPSCs. As we know, the orientation and three-dimensional structure of RGD containing peptide exhibit apparent influence on their bioactivity [55]. PDA coating with strong covalent graft ability could react with amino groups on the side-chains of VN peptide, resulting in decreased bioactivity of VN peptide. Nevertheless, the relatively weak covalent graft ability of activated PDA-CMC by NHS/EDC chemistry did not affect the bioactivity of VN peptide. This is consistent with previously reported acrylate [26] and SIP [24,30] surfaces that could support the self-renewal of hPSCs after being grafted with adhesive peptides. Moreover, we think the peptide bond structure that formed between PDA-CMC and VN peptide is beneficial to retain the bioactivity of VN peptide.

AFM measurement also demonstrated that PDA-CMC-VN surface not only exhibited appropriate nanotopography (Z = 24.1 nm and Ra = 2.2 nm at 1 μm × 1 μm; Z = 113 nm and Ra = 2.4 nm at 5 μm × 5 μm) for the adhesion and proliferation of hPSCs (Fig. 1d) [56], but also endowed the stiff cell culture plates with soft surface (Young's modulus = 5.58 MPa at 1 μm × 1 μm; Young's modulus = 4.82 MPa at 5 μm × 5 μm) that was beneficial to the homogeneous self-renewal of hPSCs (Fig. S6) [57]. Moreover, knowing that the distribution of VN peptide on PDA-CMC-VN surface has great implications for adhesion and self-renewal of hPSCs, FITC-labeled VN peptide was conjugated to PDA-CMC decorated 6-well cell culture plates as previously described. Then, a large fluorescent image at a size of 1.5 cm × 1.5 cm that composed of 361 pictures was made using LSM5 laser confocal microscopy (Carl Zeiss, Germany) with the excitation wavelength at 488 nm. Make clear that the lower fluorescence intensity in the bottom right corner of each picture was caused by the imperfection of laser confocal microscopy, the difference of fluorescence intensity for all 361 pictures on PDA-CMC-VN surface were little (Fig. S7a). CMC, one of chitosan derivatives from animal chitin, has been commonly applied as a promising biopolymer for drug delivery systems and tissue engineering scaffolds with the advantages of enhanced aqueous solubility, excellent biocompatibility, and controllable biodegradability. These features make it desirable for use in hPSCs culture [58].

Knowing that the cell numbers of H1 hESCs and hNF-C1 hiPSCs as single cells at day 4 on PDA-CMC-VN surface were much less than those on Matrigel (Fig. 1b), we have investigated the effect of peptide concentration, dissociation method and ROCK inhibitor Y-27632 on the cell binding capacity of PDA-CMC-VN surface in mTeSR1 medium. As shown in Fig. 1e, a good correlation was found between conjugated VN peptide density and hNF-C1 hiPSCs cell numbers after 4 day of culture on PDA-CMC-VN surface. The cell number of H1 hESCs increased evidently with the enrichment of VN peptide from 0.25 mM to 0.75 mM. These results reveal that high surface density of the supportive peptide on PDA-CMC-VN is required to achieve hPSCs expansion. EDTA dissociation method and Y-27632 that exhibit great benefits to the survival of hPSCs were applied to facilitate the attachment and growth of H1 hESCs and hNF-C1 hiPSCs on PDA-CMC-VN surface (Fig. 1f) [59,60]. Regardless of whether hPSCs were dissociated as single cells or colonies, supplement of 5 μM Y-27632 for 1 day had apparently increased the cell numbers of both H1 hESCs and hNF-C1 hiPSCs at day 4 on PDA-CMC-VN surface ($p < 0.05$). However, either seeding as single cells or colonies on Matrigel surface, the promoting effect of Y-27632 was only found for the survival of H1 hESCs, but not for hNF-C1 hiPSCs. Moreover, in the presence of Y-27632 or not, the cell numbers of H1 hESCs and hNF-C1 hiPSCs that dissociated as colonies were much more than those dissociated as single cells after 4 day of culture on PDA-CMC-VN surface ($p < 0.05$). Surprisingly, it was found that when seeding hPSCs as colonies with the supplementation of Y-27632, the cell numbers of H1 hESCs and hNF-C1 hiPSCs after 4 days in culture on PDA-CMC-VN surface were very close to those on Matrigel surface, indicating they exhibited comparable properties in hPSCs proliferation. Moreover, similar results were found when the medium was changed to E8 (Fig. S8a–c). Besides, except for the marginal area, we observed uniform distributed H9 hESCs colonies on PDA-CMC-VN surface after 2 day of culture in mTeSR1 medium (Fig. S7b), indicating whole PDA-CMC-VN surface on cell culture plates presented enough VN peptide for the survival of hPSCs. As a matter of fact, more hPSCs colonies adhesion on the marginal area were also found in our daily cultivation of hPSCs on Matrigel surface, which supposed due to the edge effect.

H1 hESCs in mTeSR1 medium were seeded onto PDA-CMC-VN and Matrigel surface as single cells, and the cell attachment was investigated by live cell images at time intervals of 1 h, 4 h, 12 h and 24 h (Fig. 1g). Well-spread single H1 hESCs were observed on Matrigel surface after 1 h of culture, but not on PDA-CMC-VN surface. When cultured for 4 h, the cell migration of H1 hESCs on Matrigel surface was more apparent than that on PDA-CMC-VN surface. Then, bigger H1 hESCs colonies were found on Matrigel surface in comparison with PDA-CMC-VN surface after both 12 h and 24 h of seeding. Compared to Matrigel, a gelatinous protein mixture that secreted by the sarcoma cells of Engelbreth-Holm-Swarm (EHS) mouse, PDA-CMC-VN surface is not beneficial to the adhesion of hPSCs, which is the reason why the cell numbers of hPSCs that seeded onto PDA-CMC-VN surface as colonies with the supplementation of Y-27632 for 4 days are slightly less than Matrigel control.

3.2. Genome-wide gene profiling analysis

To gain insights of the mechanism underlying the cell-adhesion process, we performed RNA-seq to compare the gene expression patterns of hPSCs cultured on PDA-CMC-VN and Matrigel surface. We found that hPSCs cultured on PDA-CMC-VN surface had gene expression profile closely resembling those on Matrigel surface. H1 hESCs and hNF-C1 hiPSCs cultured on PDA-CMC-VN surface clustered together with their control on Matrigel surface, respectively ($R > 0.97$, Fig. 2a). Among differentially expressed genes, 735 and 317 genes were expressed at lower level in H1 hESCs and hNF-C1 hiPSCs on PDA-CMC-VN surface than cells on Matrigel surface

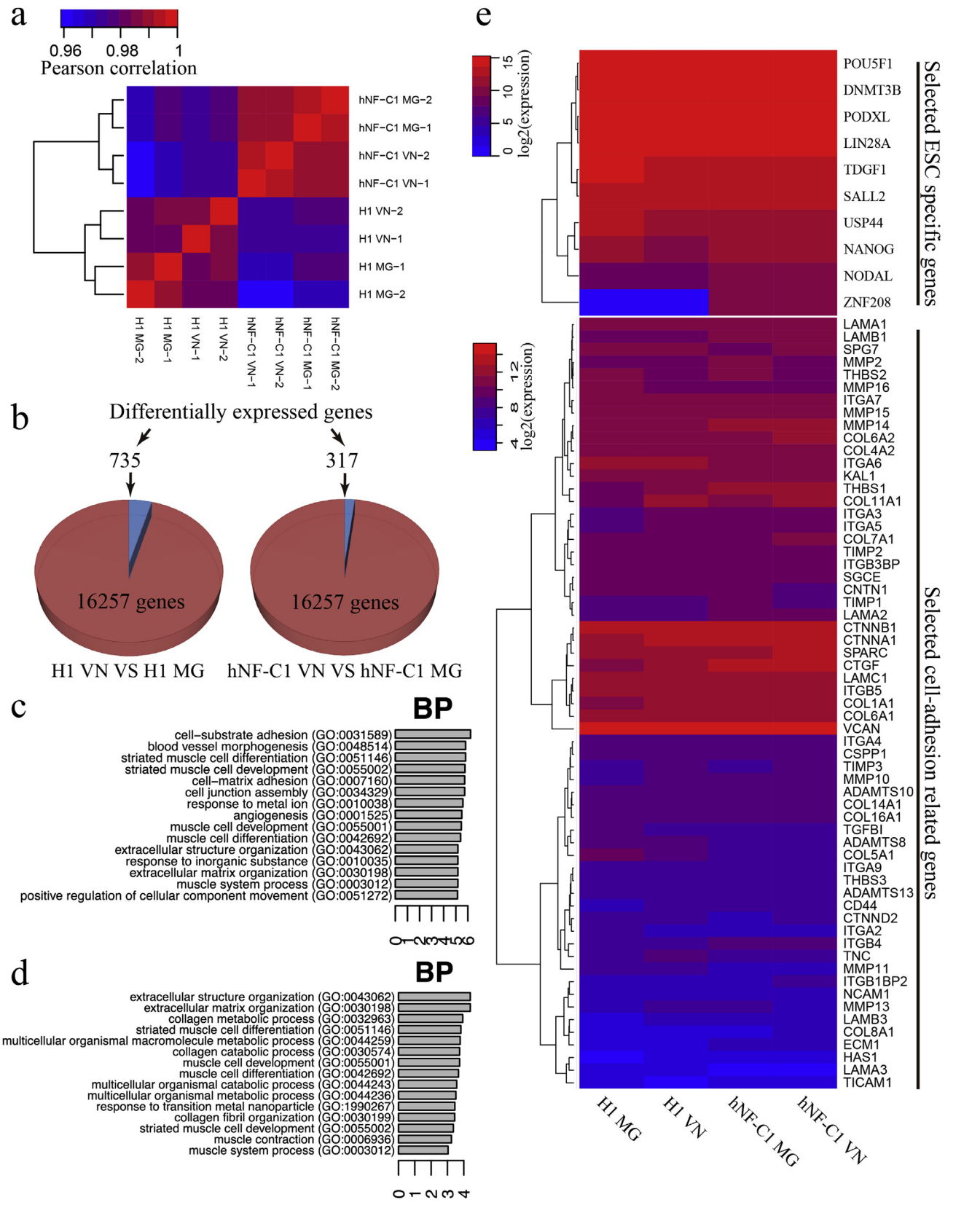

Fig. 2. Global gene expression analysis of hPSCs on PDA-CMC-VN and Matrigel surface. (a) Pearson correlation analyses of global gene expression in H1 hESCs and hNF-C1 hiPSCs that attached on PDA-CMC-VN and Matrigel surface for 24 h. (b) Pie charts show the number of differentially expressed genes with an adjusted P value 0.05 and fold change 2 in hPSCs on PDA-CMC-VN and Matrigel surface. (c–d) Functional annotations of these differentially expressed genes in H1 hESCs (c) and hNF-C1 hiPSCs (d) samples. Gene ontology (GO) statistics for these genes were computed using the hypergeometric test, and down-regulated GO terms (biological processes) for each cell type were plotted with $-\log_{10}$ of the adjusted P values (adjpvalue). (e) Heatmap displays the expression profile of selected embryonic stem cell specific genes and cell-adhesion related genes for those hPSCs samples. The mean expression values of two duplicate samples for each group were applied for the heatmap analysis.

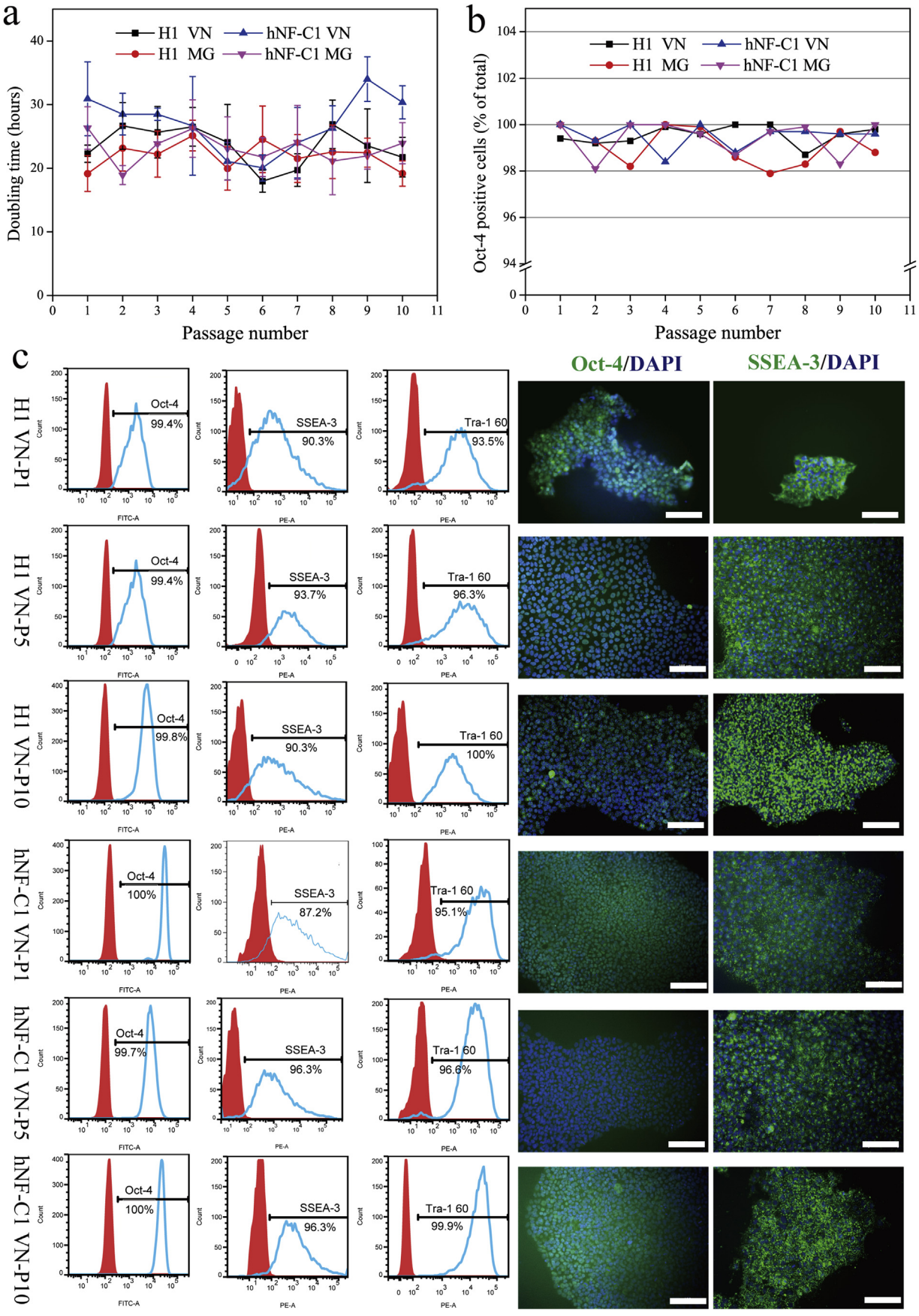
a
H1 VN
hNF-C1 VN
H1 MG
hNF-C1 MG
Doubling time (hours)
Passage number
b
Oct-4 positive cells (% of total)
Passage number
c
Oct-4/DAPI
SSEA-3/DAPI
H1 VN-P1
Oct-4 99.4%
SSEA-3 90.3%
Tra-1 60 93.5%
H1 VN-P5
Oct-4 99.4%
SSEA-3 93.7%
Tra-1 60 96.3%
H1 VN-P10
Oct-4 99.8%
SSEA-3 90.3%
Tra-1 60 100%
hNF-C1 VN-P1
Oct-4 100%
SSEA-3 87.2%
Tra-1 60 95.1%
hNF-C1 VN-P5
Oct-4 99.7%
SSEA-3 96.3%
Tra-1 60 96.6%
hNF-C1 VN-P10
Oct-4 100%
SSEA-3 96.3%
Tra-1 60 99.9%
FITC-A
PE-A
Count

respectively (Fig. 2b, Fig. S9a–b). GO biological process analysis of these genes is shown in Fig. 2c–d. Compared to Matrigel control, genes involving in extracellular structure organization and extracellular matrix organization were downregulated for both H1 hESCs and hNF-C1 hiPSCs seeded on PDA-CMC-VN surface. This may be due to longer time needed for the adherence of hPSCs to PDA-CMC-VN surface in comparison to Matrigel surface, so activation of extracellular matrix secretion occurred later. However, only H1 hESCs cultured on PDA-CMC-VN surface were found to express genes related to cell-substrate adhesion and cell-matrix adhesion at lower level compared to their counterparts on Matrigel surface. This could explain why the cell number of H1 hESCs seeded as colonies was lower than hNF-C1 hiPSCs on the same PDA-CMC-VN surface without the addition of Y-27632 (Fig. 1f). Notably, genes involved in development of striated muscle cell and muscle cell were also lowly expressed in these hPSCs on PDA-CMC-VN surface (Fig. 2c–d), indicating our synthetic surface is beneficial for the self-renewal of hPSCs, although it may also imply PDA-CMC-VN surface affect muscle development. Moreover, the expression pattern of crucial pluripotency genes for H1 hESCs on PDA-CMC-VN surface was similar to that on Matrigel surface, and no significant difference of such genes was found for hNF-C1 hiPSCs (Fig. 2e, upper panel). This result suggests that PDA-CMC-VN surface is comparable to Matrigel surface in supporting the pluripotency maintenance of hPSCs. Importantly, we also noted that a few genes related to cell-adhesion were upregulated in hPSCs on PDA-CMC-VN surface in comparison to Matrigel surface (Fig. 2e, lower panel). Compared to control cultured on Matrigel, cell-adhesion related genes such as CTGF, COL11A1, THBS1 for H1 hESCs and COL11A1, COL7A1 for hNF-C1 hiPSCs were upregulated more than two fold (Fig. S9c). This data prove that our synthetic surface is better than Matrigel to support expression of certain genes involved in cell adhesion, although hPSCs cultured on PDA-CMC-VN surface expressed substantial of genes associated with extracellular matrix formation and cell-adhesion at lower level in general. Together these data showed that the ability of PDA-CMC-VN surface to maintain pluripotency of hPSCs was comparable to Matrigel control, although subtle difference remained for cell-adhesion.

Moreover, H1 hESCs and hNF-C1 hiPSCs were seeded as colonies onto PDA-CMC-VN and Matrigel coated glass-bottom dishs for 24 h. Then, both for H1 hESCs and hNF-C1 hiPSCs, we found that the expression of Vinculin, a membrane-cytoskeletal protein in focal adhesion plaque that play a key role in hPSCs adhesion, on PDA-CMC-VN and Matrigel surface were similar as shown by immunostaining (Fig. S10). This indicated that hPSCs on synthetic PDA-CMC-VN surface exhibited comparable ability in production of focal adhesion plaque to Matrigel control. These results of RNA-seq and immunostaining suggested that our PDA-CMC-VN can be used for the long-term self-renewal of hPSCs.

3.3. Detailed evaluation of hPSCs proliferation and pluripotency in ten passages

H1 hESCs and hNF-C1 hiPSCs were serially passaged on both PDA-CMC-VN and Matrigel surface in mTeSR1 medium for ten passages, and their proliferation rates and pluripotency maintenance were investigated in detail. The cells doubling times of hPSCs were assessed at each passage for ten passages (Fig. 3a). Both for H1 hESCs and hNF-C1 hiPSCs, doubling times for cells grown on PDA-CMC-VN surface were similar to those of Matrigel cultures, proving the growth rates of hPSCs cultured on PDA-CMC-VN surface were comparable to those of Matrigel control. In addition, at each passage of ten passages, FACS analysis indicated that more than 97.9% of hPSCs grown on both PDA-CMC-VN and Matrigel surface were positive in Oct-4 expression (Fig. 3b). Moreover, we measured the expression of SSEA-3 and Tra-1 60 for hPSCs grown on PDA-CMC-VN and Matrigel surface at P1, P5 and P10 using FACS too. At least 80.0% of these cell samples positively expressed SSEA-3, and 91.8% for Tra-1 60 (Fig. 3c, left; Fig. S11, left). Furthermore, all for H1 hESCs and hNF-C1 hiPSCs cultured on PDA-CMC-VN and Matrigel surface at P1, P5 and P10, immunofluorescence analysis shown that Oct-4 and SSEA-3 were expressed at high levels throughout the colonies (Fig. 3c, right; Fig. S11, right). These measurements demonstrate that PDA-CMC-VN surface is comparable to Matrigel surface in terms of pluripotency maintenance for hPSCs.

Moreover, after serially passaged on PDA-CMC-VN surface in E8 for 10 passages, H1 hESCs showed unaltered morphology (Fig. S8d) with intact karyotype (Fig. S8e). Immunofluorescence showed that Oct-4 and SSEA-3 were expressed at high levels throughout the colonies (Fig. S8f). FACS analysis indicated that most cells co-expressed pluripotent markers such as Oct-4, SSEA-3, and Tra-1 60 (Fig. S8g). Quantitative RT-PCR demonstrated the formation of cells from all three germ layers in EBs from H1 hESCs samples (Fig. S8j). These results suggested that our PDA-CMC-VN surface could also support the self-renewal of hPSCs using xeno-free E8 medium.

3.4. Derivation of hiPSCs on PDA-CMC-VN surface

Mostly, hiPSCs were generated from various human somatic cells on feeder cell layers, Matrigel, proteins and protein fragments that support the survival of hPSCs. So far, none of synthetic peptide presenting surfaces have been reported to support the derivation of hiPSCs, and the question arose that whether the reprogramming of human somatic cells could be accomplished on these artificial surfaces. Taking surface-initiated polymerization (SIP), a common surface modification method to present carboxyl group on substrate surface, as an example, it has been used to conjugate various peptides for the self-renewal of hPSCs for years, but none had investigated whether these surfaces could support human somatic cells reprogramming or not. Thus, we performed the reprogramming of both human urine derived cells (hUC) and human umbilical cord blood cells (hUMC) on Au-SIP-VN surface [30], and found that no ESC-like hiPSCs colonies appeared (Fig. S12). This indicates that surface suitable for long-term self-renewal of hPSCs may not fit for somatic cell reprogramming.

Fortunately, we generated four hiPSCs lines from 2 donors of hUC and 2 donors of hUMC on our PDA-CMC-VN surface under defined conditions (Fig. 4). When reprogramming for about 3 weeks, many typically ESC-like hiPSCs colonies could be observed evidently on PDA-CMC-VN surface (Fig. S13b). For all these four acquired hiPSCs lines, cells presented typically undifferentiated morphologies (Fig. S13c), and with intact karyotypes (Fig. 4a, left). Moreover, they expressed high levels of pluripotency markers such

Fig. 3. Evaluation of proliferation and pluripotency for H1 hESCs and hNF-C1 hiPSCs cultured on PDA-CMC-VN and Matrigel surface for ten passages. (a) Cell doubling times of H1 hESCs and hNF-C1 hiPSCs over the course of 10 consecutive passages on PDA-CMC-VN and Matrigel surface. (b) Oct-4 expression of H1 hESCs and hNF-C1 hiPSCs cultured on PDA-CMC-VN and Matrigel surface for 10 sequential passages measured by FACS. (c) FACS analysis of Oct-4, SSEA-3 and Tra-1 60 for H1 hESCs and hNF-C1 hiPSCs cultured on PDA-CMC-VN surface at P1, P5 and P10. IgG and IgM control: red peak; FITC or PE-conjugated antibody: unfilled peak. To the right, immunostaining of Oct-4 (green) and SSEA-3 (green) for those cells are shown. Nuclei were visualized by DAPI-staining (blue). Scale bars, 100 μm. (For interpretation of the references to color in this figure legend, the reader is referred to the web version of this article.)

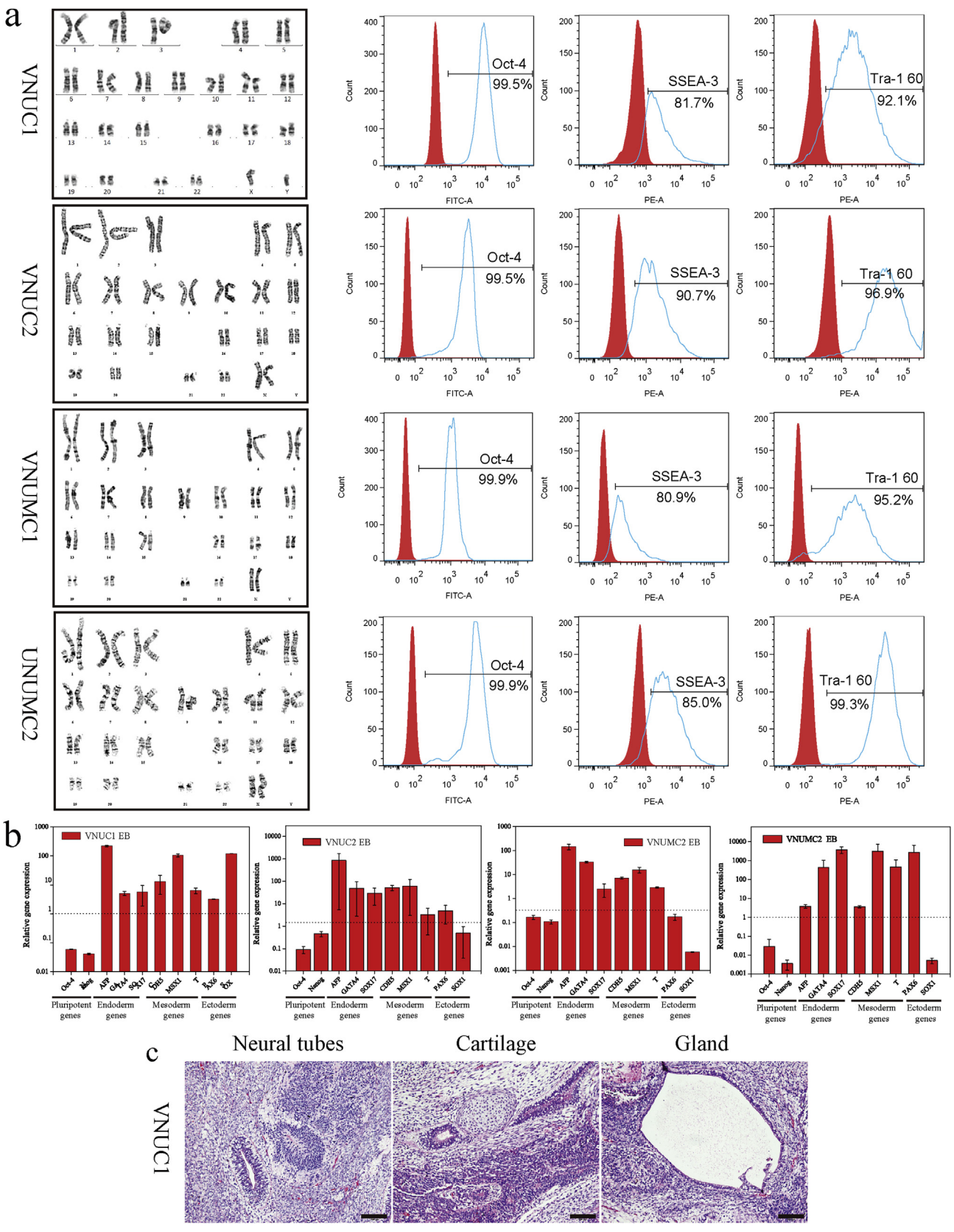

Fig. 4. Generation of hiPSCs from hUC and hUMC on PDA-CMC-VN surface. (a) Karyotypes (left) and expressions of protein markers (Oct-4, SSEA-3 and Tra-1 60) measured using FACS analysis (right) for hiPSCs derived from both 2 donors of hUC and hUMC on PDA-CMC-VN surface. (b) Quantitative RT-PCR was performed in spontaneously differentiated cells derived from these hiPSCs to detect expression of three-germ layer gene markers (ectoderm: PAX6 and Sox1; mesoderm:T, MSX1 and CDH5; endoderm: AFP, GATA4 and SOX17). The expression of these genes in hPSCs before differentiation has been standardized to 1, and it is marked by a single dotted threshold line. (k) VNUC1 hiPSCs were injected subcutaneously into SCID mice to form a teratoma, and pluripotency was determined by tissues from all three germ layers, represented as secretory epithelium (endoderm), cartilage (mesoderm) and neuroepithelium (ectoderm). Scale bars: 200 μm.

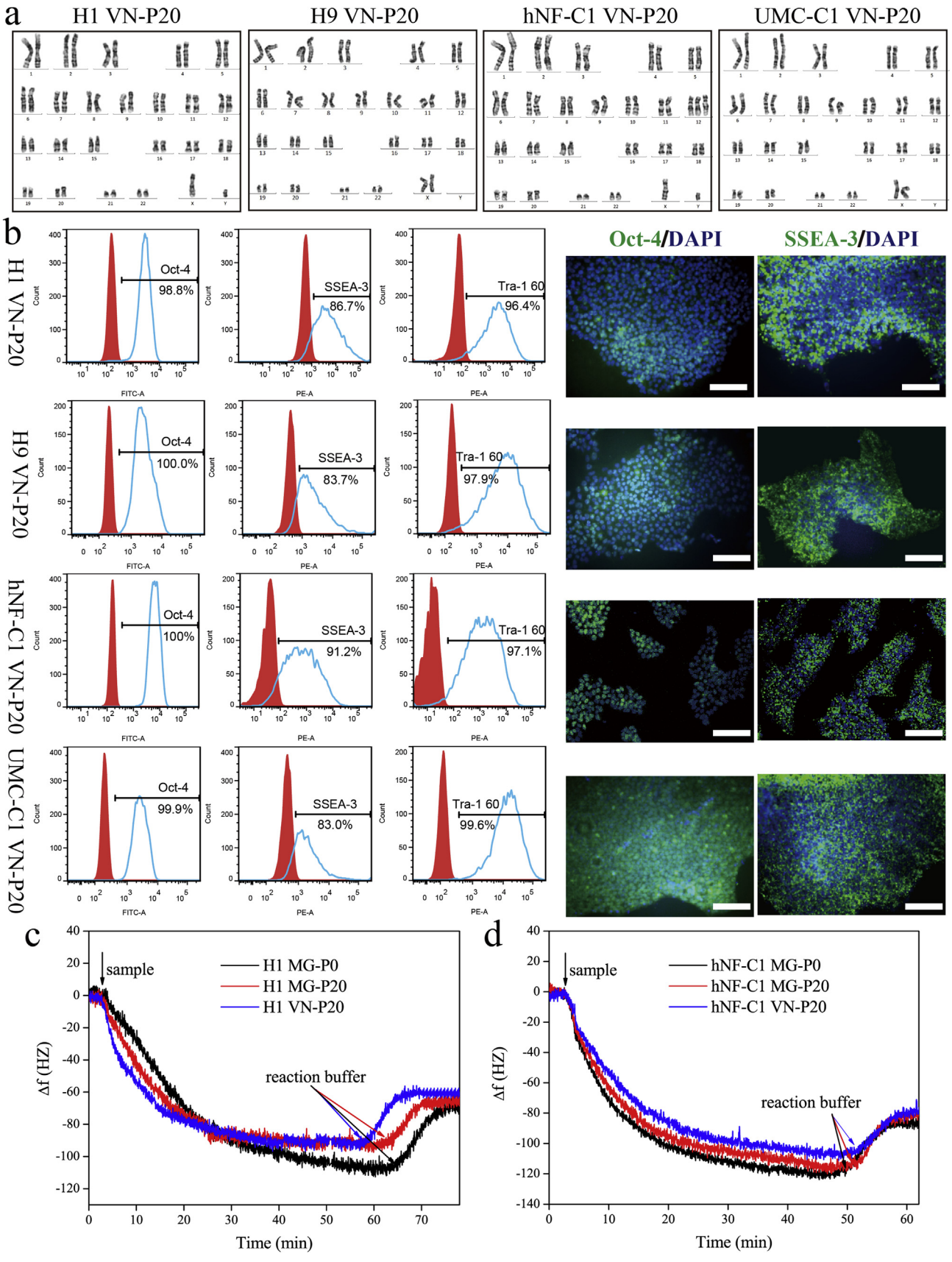

Fig. 5. Long-term self-renewal of hPSCs on PDA-CMC-VN surface. (a) Karyotype analysis of four hPSCs lines (H1 hESCs, H9 hESCs, hNF-C1 hiPSCs, and UMC-C1 hiPSCs) after cultured on PDA-CMC-VN surface for 20 passages. (b) FACS measurements of Oct-4, SSEA-3 and Tra-1 60 for all four hPSCs lines samples. IgG and IgM control: red peak; FITC or PE-conjugated antibody: unfilled peak. To the right, immunostaining of Oct-4 (green) and SSEA-3 (green) for those cells are shown. Nuclei were visualized by DAPI-staining (blue). Scale bars, 100 μm. (c–d) Telomerase activity of H1 hESCs (c) and hNF-C1 hiPSCs (d) before and after 20 passages on Matrigel and PDA-CMC-VN surface. (For interpretation of the references to color in this figure legend, the reader is referred to the web version of this article.)

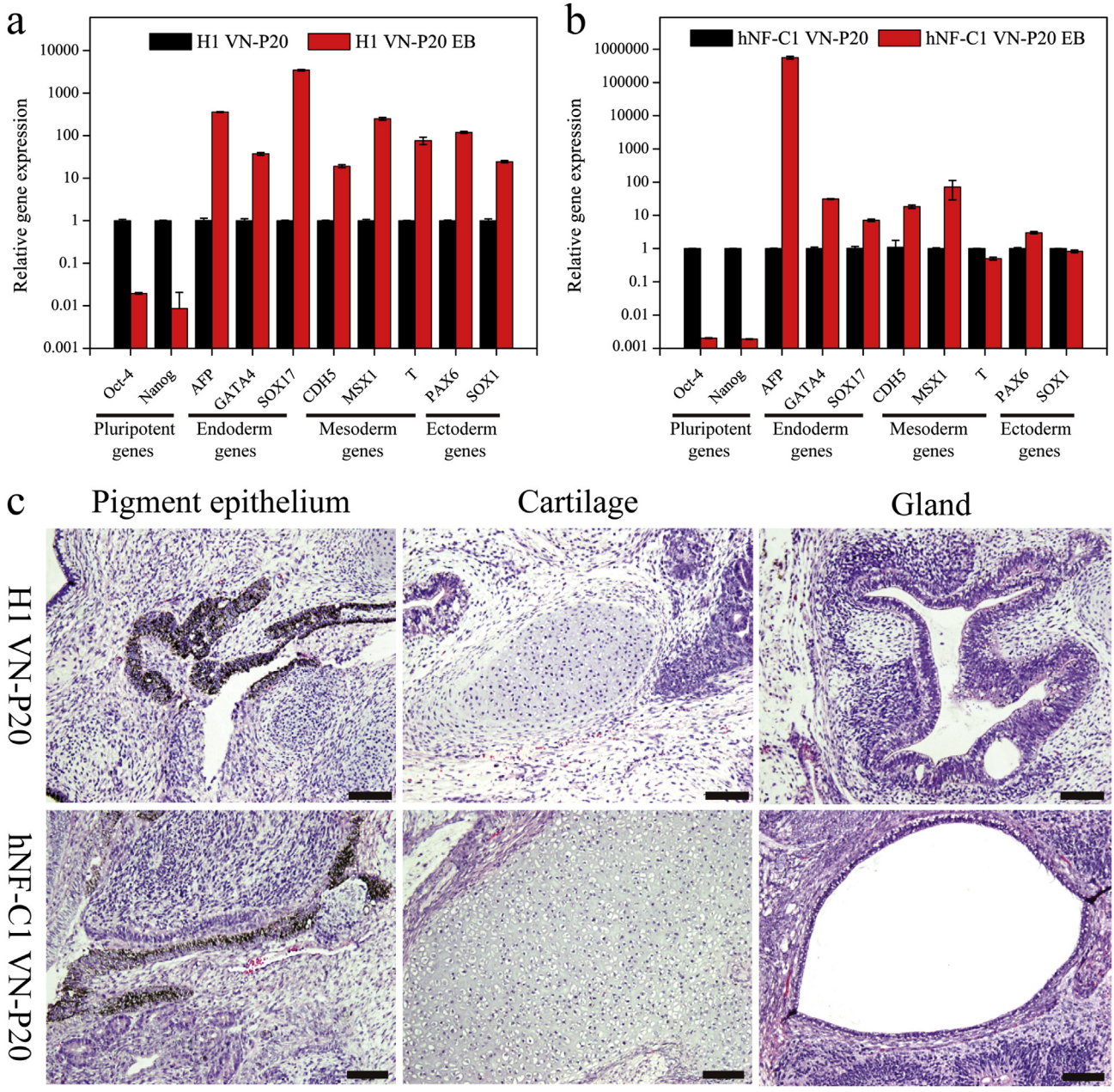

Fig. 6. Multipotent differentiation of hPSCs on PDA-CMC-VN surface. (a–b) Quantitative RT-PCR results for the relative expression of three-germ layer gene markers for spontaneous differentiated H1 hESCs (a) and hNF-C1 hiPSCs (b) both at P20 on PDA-CMC-VN surface. The expression of these genes in hPSCs before differentiation has been standardized to 1, which is marked by a single dotted threshold line as indicated. (c) Tissues from all three germ layers, represented as secretory epithelium (endoderm), cartilage (mesoderm) and neuroepithelium (ectoderm), were identified in teratomas formed by H1 hESCs and hNF-C1 hiPSCs cultured on PDA-CMC-VN surface for 20 passages. Scale bars, 200 μm.

as Oct-4, SSEA-3 and Tra-1 60, as shown by FACS analysis (Fig. 4a, right) and immunostaining (Fig. S13d). Furthermore, *in vitro* EB and *in vivo* teratoma formation proved that all four hiPSCs lines could generate all three germ layers cells (Fig. 4b–c). To our knowledge, these results, for the first time, have demonstrated that multiple human somatic cells could be successfully reprogrammed into hiPSCs on synthetic peptide presenting surface under defined conditions, which would promote the application of synthetic surfaces in hiPSCs studies.

The reprogramming of hUC and hUMC on Au-SIP-VN and PDA-CMC-VN surface revealed that peptide-conjugated synthetic surfaces that allow the survival of hPSCs may not support the generation of hiPSCs. The same with PDA-CMC-VN surface, we previously found that the cell number of hPSCs after 3 day of culture on Au-SIP-VN surface in mTeSR1 medium was similar to Matrigel control [30]. This indicate that the density and presentation of VN peptide on Au-SIP-VN and PDA-CMC-VN surface should have no significant difference. It is reported that softer substrate is beneficial in cellular reprogramming through mesenchymal-to-epithelial transition and stemness markers expression [61]. We found that the elasticity modulus and hardness of Au-SIP-VN were much higher than those of PDA-CMC-VN surface (Table S2), which may be the reason why human urine derived cells and human umbilical cord blood cells could reprogrammed into hiPSCs on PDA-CMC-VN surface, but not on Au-SIP-VN surface.

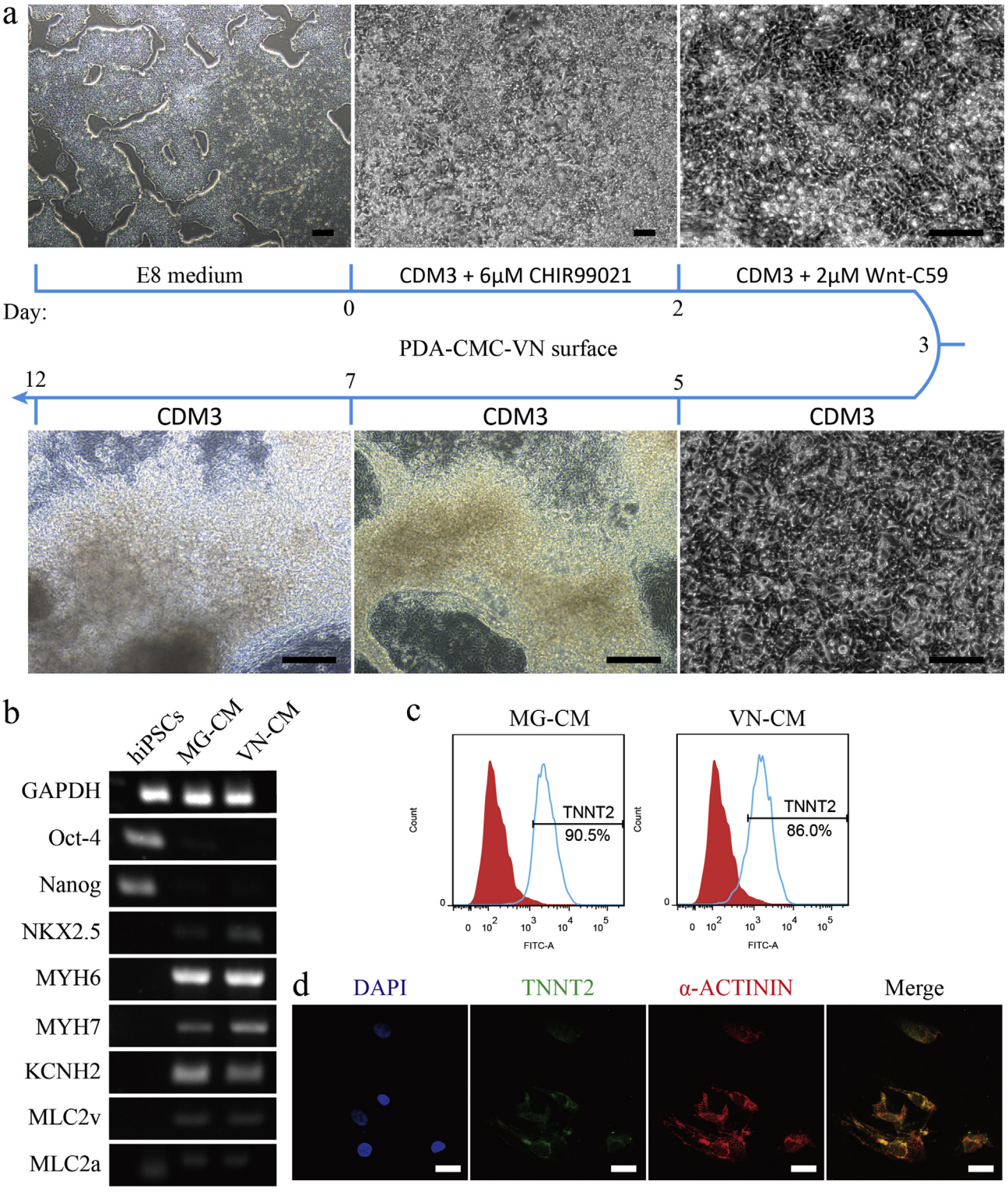

Fig. 7. Directed differentiation of hNF-C1 hiPSCs into cardiomyocytes on PDA-CMC-VN surface. (a) Cell morphologies of hNF-C1 hiPSCs on PDA-CMC-VN surface before and after induction for various days (2, 3, 5, 7 and 12 days). (b) RT-PCR analysis of RNAs from differentiated cardiomyocytes on PDA-CMC-VN (VN-CM) and Matrigel (MG-CM) surface illustrating the expression of pluripotent genes (Oct-4 and Nanog), and cardiomyocyte-specific genes (NKX2.5, MYH6, MYH7, KCNH2, MLC2v and MLC2a). Gene expression of undifferentiated hNF-C1 hiPSCs on Matrigel surface served as the control. (c) Flow cytometry analysis based on TNNT2 staining for differentiated cardiomyocytes on PDA-CMC-VN (VN-CM) and Matrigel (MG-CM) surface. (d) Immunofluorescence staining for TNNT2 and α-ACTININ for cardiomyocytes on PDA-CMC-VN surface. Black scale bars: 200 μm. White scale bars: 20 μm.

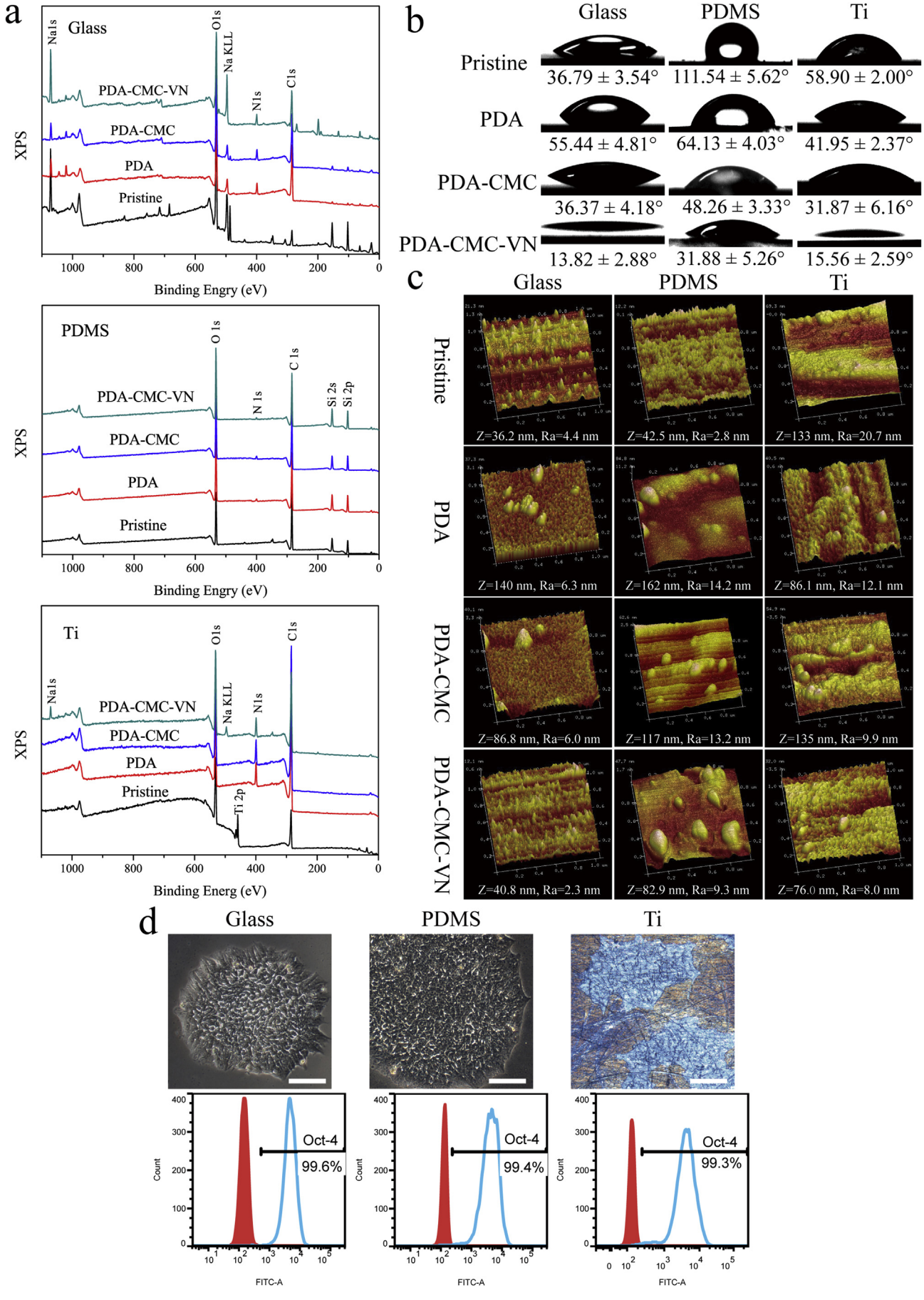
a
Glass
Na1s
O1s
Na KLL
N1s
C1s
PDA-CMC-VN
PDA-CMC
PDA
Pristine
XPS
1000 800 600 400 200 0
Binding Engry (eV)
PDMS
O 1s
C 1s
N 1s
Si 2s
Si 2p
PDA-CMC-VN
PDA-CMC
PDA
Pristine
XPS
1000 800 600 400 200 0
Binding Engry (eV)
Ti
Na1s
O1s
Na KLL
N1s
C1s
Ti 2p
PDA-CMC-VN
PDA-CMC
PDA
Pristine
XPS
1000 800 600 400 200 0
Binding Energ (eV)
b
Glass
PDMS
Ti
Pristine
36.79 ± 3.54°
111.54 ± 5.62°
58.90 ± 2.00°
PDA
55.44 ± 4.81°
64.13 ± 4.03°
41.95 ± 2.37°
PDA-CMC
36.37 ± 4.18°
48.26 ± 3.33°
31.87 ± 6.16°
PDA-CMC-VN
13.82 ± 2.88°
31.88 ± 5.26°
15.56 ± 2.59°
c
Glass
PDMS
Ti
Pristine
Z=36.2 nm, Ra=4.4 nm
Z=42.5 nm, Ra=2.8 nm
Z=133 nm, Ra=20.7 nm
PDA
Z=140 nm, Ra=6.3 nm
Z=162 nm, Ra=14.2 nm
Z=86.1 nm, Ra=12.1 nm
PDA-CMC
Z=86.8 nm, Ra=6.0 nm
Z=117 nm, Ra=13.2 nm
Z=135 nm, Ra=9.9 nm
PDA-CMC-VN
Z=40.8 nm, Ra=2.3 nm
Z=82.9 nm, Ra=9.3 nm
Z=76.0 nm, Ra=8.0 nm
d
Glass
PDMS
Ti
Count
Oct-4
99.6%
99.4%
99.3%
FITC-A

3.5. Pluripotency of hPSCs after 20 passages on PDA-CMC-VN surface

Two hESCs lines (H1 and H9) and two hiPSCs lines (hNF-C1 and UMC-C1) were sequentially passaged on PDA-CMC-VN surface in defined mTeSR1 medium for over 20 passages with Matrigel as a control, in order to determine whether the synthetic surface could support the long-term self-renewal of hPSCs. All hPSCs on PDA-CMC-VN surface at P20 showed unaltered morphology (Fig. S14), and their karyotypes remained intact (Fig. 5a). FACS analysis indicated that most hPSCs cultured on PDA-CMC-VN surface co-expressed pluripotent markers such as Oct-4, SSEA-3, and Tra-1 60. Immunofluorescence showed that Oct-4 and SSEA-3 were expressed at high levels throughout the colonies (Fig. 5b). These results agreed perfectly with that of the control group (Fig. S15, Fig. S16a–b). Besides, these four hPSCs lines maintained in the frozen stock solution could be thawed and used for fresh cultures on PDA-CMC-VN surface (Fig. S17).

It is known that high telomerase activity in pluripotent stem cell correlates with their ability to self-renewal [62]. However, the telomerase activity of hPSCs after long-term self-renewal on synthetic surfaces had never been studied. Interestingly, the telomerase activity of hNF-C1 hiPSCs ($\Delta f = 88$ HZ) is a little higher than that of H1 hESCs ($\Delta f = 72$ HZ) at 0th generation on Matrigel surface measured by quartz crystal microbalance (QCM) (Fig. 5d). The telomerase activities of H1 hESCs and hNF-C1 hiPSCs after 20 passages on both Matrigel and PDA-CMC-VN surface were in close vicinity to cells at P0. It demonstrates that hPSCs cultured on PDA-CMC-VN surface retained as good telomerase activity as on Matrigel surface.

Moreover, we further analyzed the pluripotency of H1 hESCs and hNF-C1 hiPSCs on PDA-CMC-VN surface at P20 using *in vitro* embryoid body (EB) and *in vivo* teratoma formation, since maintenance of multipotent differentiation ability play a key role in evaluating new culture surface. Quantitative RT-PCR demonstrated the formation of cells from all three germ layers in EBs from those hPSCs samples (Fig. 6a–b), which is consistent with Matrigel control (Fig. S16c–d). Moreover, teratoma formation assay showed that cells could form teratoma after 6–8 weeks, and generate cells derived from all three germ layers (Fig. 6c). These results demonstrated that hPSCs retained the multilineage potential after cultured on PDA-CMC-VN surface for 20 passages.

3.6. In vitro differentiation of hPSCs on PDA-CMC-VN surface

Spontaneously beating clusters were observed from day 9 after cardiac induction on PDA-CMC-VN surface (Movie S1). At 12 day of differentiation, we accessed the differentiation efficiency of hNF-C1 hiPSCs on both PDA-CMC-VN (86%) and Matrigel (90.5%) surface as measured by FACS for TNNT2 (Fig. 7c). Furthermore, we examined the expression of both pluripotent and cardiomyocyte specific genes by RT-PCR (Fig. 7b). As expected, the pluripotent genes Oct-4 and Nanog were down-regulated and the early heart development related gene NKX2.5 was up-regulated. Consistently, the differentiated cells expressed cardiomyocyte specific genes such as MYH6, MYH7, MLC2a, MLC2v and KCNH2, indicating that these cardiomyocytes containing subtypes of atrial-like cells (MLC2a) and ventricular-like cells (MLC2v). We noted that cells differentiated on PDA-CMC-VN surface expressed higher NKX2.5, MYH6 and MYH7 than Matrigel group, suggesting that PDA-CMC-VN surface may be more favorable for the maturation of hiPSCs derived cardiomyocytes compared with Matrigel surface. Besides, functional cardiomyocytes on PDA-CMC-VN surface positively expressed TNNT2 and α-ACTININ as confirmed by immunofluorescence staining (Fig. 7d).

Supplementary data related to this article can be found online at http://dx.doi.org/10.1016/j.biomaterials.2016.02.012.

Moreover, uniform EBs were generated from H9 hESCs at P15 on PDA-CMC-VN surface using AggreWell™800 plates (Fig. S18a), and then differentiated towards neural cells under defined conditions. We observed some neural rosette structures in neural aggregates after incubating in neural induction medium for 14 days (Fig. S18b). Cells expressed neural markers such as Sox-1 and Nestin (Fig. S18d), demonstrating the successful generation of neural progenitor cells. Then, we collected those neural rosette structures and cultured in neural rosette selection reagent for 7 days to further differentiate into neurons (Fig. S18c), which were proved by the expression of neuron markers such as MAP-2 and TUJ-1 via immunofluorescence (Fig. S18e).

These results proved the capacity of hPSCs to differentiate into cardiomyocytes and neural cells on PDA-CMC-VN surface, confirming that the surface is suitable for both the expansion and differentiation phases of hPSC culture.

3.7. hPSCs cultured on diverse substrates with PDA-CMC-VN surface

Taking the advantage of polydopamine, our PDA-CMC-VN surface could support the growth of hPSCs on diverse solid substrates. In this regard, we modified glass (basic materials for optical imaging research), PDMS (hydrophobic and anti-fouling materials widely used in the fields of microfluidics and patterned surface [63,64]) and Ti (mostly used as biomaterials for implants) with PDA-CMC-VN surface for the adhesion and growth of hPSCs.

The alterations of chemical composition and surface morphology after each modification step on glass, PDMS and Ti substrates were analyzed by XPS, water contact angle and AFM. XPS measurement of PDA-CMC-VN surface on these substrates was similar to that on PS. Briefly, newly detected N 1 s peaks in the wide spectra of PDA decorated surfaces and broad -C-N- peaks in the high-resolution C 1 s spectrums of PDA-CMC coated surfaces demonstrated PDA and CMC were grafted on those substrates (Fig. 8a, Fig. S19c, Fig. S20c, Fig. S21c). Then, the conjugation of VN peptides on those substrates was proved by the enhanced peaks of −C═O and -C-N- in high-solution C 1 s spectrum and the content of N element alteration (Fig. S19d–e, Fig. S20d–e, Fig. S21d–e).

Prior to modification, the water contact angles of pristine glass, PDMS and Ti were 36.79 ± 3.54°, 111.54 ± 5.62° and 58.90 ± 2.00° respectively (Fig. 8b). Except for glass, we detected significantly lower contact angles for PDMS and Ti after PDA coating ($p < 0.05$). Then, the contact angels of these PDA coated substrates went on to decrease both after conjugated with CMC and VN peptide, and reached a quite low value at a range from 15.56° to 31.88°. This confirmed that our PDA-CMC-VN surface could change the surface properties of diverse types of materials.

Fig. 8. hPSCs cultured on diverse substrates with PDA-CMC-VN surface under defined conditions. (a) XPS wide spectra of unmodified substrates (glass, PDMS and Ti) and sequentially decorated by PDA/CMC/VN peptide. (b) The alteration of water contact angles during each step of PDA-CMC-VN surface coating process on diverse substrates (Glass, PDMS and Ti). (c) AFM surface topographies of various substrates (glass, PDMS and Ti) before and after sequential modified by PDA/CMC/VN peptide with scan area of 1 μm × 1 μm. Insert are values of Z range and Ra for surfaces of those samples. (d) Cell colony morphology and Oct-4 expression analyzed by FACS for hNF-C1 hiPSCs cultured for 3–4 days on PDA-CMC-VN coated glass, PDMS and Ti as indicated. Scale bar, 100 μm. IgG control: red peak; FITC conjugated antibody: unfilled peak. (For interpretation of the references to color in this figure legend, the reader is referred to the web version of this article.)

We measured the surface topographies of those substrates using AFM with scan areas of 1 μm × 1 μm and 5 μm × 5 μm. For scan area of 1 μm × 1 μm (Fig. 8c), the surfaces of pristine glass (Z = 36.2 nm, Ra = 4.4 nm) and PDMS (Z = 42.5 nm, Ra = 2.8 nm) were relatively smooth. Pristine Ti exhibited rough surface (Z = 133 nm, Ra = 20.7 nm) due to the processing limits. After PDA modification, typically PDA aggregates were found and the values of Z range and Ra of glass-PDA and PDMS-PDA increased to 140/6.3 nm and 162/14.2 nm respectively. However, a more smooth surface was detected for PDA coated Ti (Ra = 12.1 nm), since grooves on the pristine Ti surface were filled with PDA particles. For all those PDA decorated substrates, the Ra values decreased both after modifying by CMC and VN peptide, and all of them terminally presented smooth surface. Similar AFM results of those substrates were measured at 5 μm × 5 μm (Fig. S22).

After incubated for 4 days, hNF-C1 hiPSCs maintained typical undifferentiated morphology on substrates (glass, PDMS and Ti) that coated by PDA-CMC-VN (Fig. 8d). Moreover, at least 99.3% of the cells on those substrates were positive for the pluripotency marker Oct-4 as detected by FACS (Fig. 8d). Remarkably, our PDA-CMC-VN surface enabled the growth of hPSCs on various substrates and possessed great prospects for further application in the fields of tissue engineering, imaging, drug screening and so on.

4. Conclusions

Herein, we have developed a synthetic PDA-CMC-VN surface, and confirmed their potential use for the generation, long-term self-renewal and differentiation of hPSCs under defined conditions. Specifically, the cell number of hPSCs that cultured on PDA-CMC-VN surface for 4 days was in close victinty to Matrigel control. The expression of cell-adhesion genes and pluripotency genes in hPSCs on the synthetic surface for 24 h was similar to that on Matrigel surface. We successfully reprogrammed human urine derived cells and human umbilical cord blood cells into hiPSCs on PDA-CMC-VN surface under defined conditions. Moreover, the proliferation rates and pluripotency maintenance of both hESCs and hiPSCs on our surface were comparable to Matrigel control throughout the long-term culture, as well as high telomerase activities. Furthermore, hPSCs were able to differentiate into cardiomyocytes and neural cells on PDA-CMC-VN surface. We also achieved the growth and proliferation of hPSCs on diverse substrates with PDA-CMC-VN surface. These results suggested that our PDA-CMC-VN surface has great value in fundamental research and clinical application of hPSCs.

Author contributions

P.Z., F.L., G.P., D.P. and S.W. conceived and designed the experiments. P.Z., F.W., T.Z., X.C., S.Z.,X.Z., Q.L., Y.L., Y.Z. and M.W. performed the experiments, P.Z. analyzed the data. P.Z. wrote the paper. All authors have given approval to the final version of the manuscript.

Acknowledgments

This work was funded by the National Natural Science Foundation of China (No. 81371697), the Open Project of Key Laboratory of Regenerative Biology (KLRB201401), and Peking University's 985 Grant. We thank Miss. Chao Xu from State Key Laboratory of Advanced Optical Communication Systems & Networks for the help of AFM measurement, Dr. Andrew Hutchins and Miss. Juan Du from Guangzhou Institutes of Biomedicine and Health for generous support in the bioinformatic analysis, as well as Miss. Caiyun Wang from Cellapybio Biotechnology Co. Ltd. for the help in cardiac differentiation.

Appendix A. Supplementary data

Supplementary data related to this article can be found at http://dx.doi.org/10.1016/j.biomaterials.2016.02.012.

References

[1] K. Takahashi, S. Yamanaka, Induction of pluripotent stem cells from mouse embryonic and adult fibroblast cultures by defined factors, Cell 126 (2006) 663–676.
[2] B.E. Reubinoff, M.F. Pera, C.Y. Fong, A. Trounson, A. Bongso, Embryonic stem cell lines from human blastocysts: somatic differentiation in vitro, Nat. Biotechnol. 18 (2000) 399–404.
[3] Kevin G. Chen, Barbara S. Mallon, Ronald D.G. McKay, Pamela G. Robey, Human pluripotent stem cell culture: considerations for maintenance, expansion, and therapeutics, Cell Stem Cell 14 (2014) 13–26.
[4] O. Genbacev, A. Krtolica, T. Zdravkovic, E. Brunette, S. Powell, A. Nath, E. Caceres, M. McMaster, S. McDonagh, Y. Li, R. Mandalam, J. Lebkowski, S.J. Fisher, Serum-free derivation of human embryonic stem cell lines on human placental fibroblast feeders, Fertil. Steril. 83 (2005) 1517–1529.
[5] I. Rodriguez-Piza, Y. Richaud-Patin, R. Vassena, F. Gonzalez, M.J. Barrero, A. Veiga, A. Raya, J.C. Izpisua Belmonte, Reprogramming of human fibroblasts to induced pluripotent stem cells under xeno-free conditions, Stem Cells 28 (2010) 36–44.
[6] J.B. Lee, J.E. Lee, J.H. Park, S.J. Kim, M.K. Kim, S. Il Roh, H.S. Yoon, Establishment and maintenance of human embryonic stem cell lines on human feeder cells derived from uterine endometrium under serum-free condition, Biol. Reprod. 72 (2005) 42–49.
[7] J. Inzunza, K. Gertow, M.A. Stromberg, E. Matilainen, E. Blennow, H. Skottman, S. Wolbank, L. Arlund-Richter, O. Hovatta, Derivation of human embryonic stem cell lines in serum replacement medium using postnatal human fibroblasts as feeder cells, Stem Cells 23 (2005) 544–549.
[8] J.A. Thomson, Embryonic stem cell lines derived from human blastocysts, Science 282 (1998) 1145–1147.
[9] C. Xu, M.S. Inokuma, J. Denham, K. Golds, P. Kundu, J.D. Gold, M.K. Carpenter, Feeder-free growth of undifferentiated human embryonic stem cells, Nat. Biotechnol. 19 (2001) 971–974.
[10] H. Bhatia, R. Sharma, J. Dawes, J.S. Khillan, Maintenance of feeder free anchorage independent cultures of ES and iPS cells by retinol/vitamin A, J. Cell. Biochem. 113 (2012) 3002–3010.
[11] M.J. Martin, A. Muotri, F. Gage, A. Varki, Human embryonic stem cells express an immunogenic nonhuman sialic acid, Nat. Med. 11 (2005) 228–232.
[12] J. Lu, R. Hou, C.J. Booth, S.H. Yang, M. Snyder, Defined culture conditions of human embryonic stem cells, Proc. Natl. Acad. Sci. U. S. A. 103 (2006) 5688–5693.
[13] S. Rodin, A. Domogatskaya, S. Strom, E.M. Hansson, K.R. Chien, J. Inzunza, O. Hovatta, K. Tryggvason, Long-term self-renewal of human pluripotent stem cells on human recombinant laminin-511, Nat. Biotechnol. 28 (2010) 611–615.
[14] N. Montserrat, E.G. Bahima, L. Batlle, S. Hafner, A.M. Rodrigues, F. Gonzalez, J.C. Izpisua Belmonte, Generation of pig iPS cells: a model for cell therapy, J. Cardiovasc. Transl. Res. 4 (2011) 121–130.
[15] G. Chen, D.R. Gulbranson, Z. Hou, J.M. Bolin, V. Ruotti, M.D. Probasco, K. Smuga-Otto, S.E. Howden, N.R. Diol, N.E. Propson, R. Wagner, G.O. Lee, J. Antosiewicz-Bourget, J.M. Teng, J.A. Thomson, Chemically defined conditions for human iPSC derivation and culture, Nat. Methods 8 (2011) 424–429.
[16] S. Wu, J. Johansson, P. Damdimopoulou, M. Shahsavani, A. Falk, O. Hovatta, A. Rising, Spider silk for xeno-free long-term self-renewal and differentiation of human pluripotent stem cells, Biomaterials 35 (2014) 8496–8502.
[17] M. Baker, Stem cells in culture: defining the substrate, Nat. Methods 8 (2011) 294–297.
[18] S.R. Braam, L. Zeinstra, S. Litjens, D. Ward-van Oostwaard, S. van den Brink, L. van Laake, F. Lebrin, P. Kats, R. Hochstenbach, R. Passier, A. Sonnenberg, C.L. Mummery, Recombinant vitronectin is a functionally defined substrate that supports human embryonic stem cell self-renewal via alpha V beta 5 integrin, Stem Cells 26 (2008) 2257–2265.
[19] A.B.J. Prowse, M.R. Doran, J.J. Cooper-White, F. Chong, T.P. Munro, J. Fitzpatrick, T.L. Chung, D.N. Haylock, P.P. Gray, E.J. Wolvetang, Long term culture of human embryonic stem cells on recombinant vitronectin in ascorbate free media, Biomaterials 31 (2010) 8281–8288.
[20] T. Miyazaki, S. Futaki, H. Suemori, Y. Taniguchi, M. Yamada, M. Kawasaki, M. Hayashi, H. Kumagai, N. Nakatsuji, K. Sekiguchi, E. Kawase, Laminin E8 fragments support efficient adhesion and expansion of dissociated human pluripotent stem cells, Nat. Commun. 3 (2012) 1236.
[21] S. Rodin, L. Antonsson, C. Niaudet, O.E. Simonson, E. Salmela, E.M. Hansson, A. Domogatskaya, Z. Xiao, P. Damdimopoulou, M. Sheikhi, J. Inzunza, A.S. Nilsson, D. Baker, R. Kuiper, Y. Sun, E. Blennow, M. Nordenskjöld, K.H. Grinnemo, J. Kere, C. Betsholtz, O. Hovatta, K. Tryggvason, Clonal culturing of human embryonic stem cells on laminin-521/E-cadherin matrix in defined and xeno-free environment, Nat. Commun. 5 (2014) 3159.

[22] H.F. Lu, C. Chai, T.C. Lim, M.F. Leong, J.K. Lim, S. Gao, K.L. Lim, A.C.A. Wan, A defined xeno-free and feeder-free culture system for the derivation, expansion and direct differentiation of transgene-free patient-specific induced pluripotent stem cells, Biomaterials 35 (2014) 2816–2826.
[23] M. Widhe, H. Bysell, S. Nystedt, I. Schenning, M. Malmsten, J. Johansson, A. Rising, M. Hedhammar, Recombinant spider silk as matrices for cell culture, Biomaterials 31 (2010) 9575–9585.
[24] J.R. Klim, L. Li, P.J. Wrighton, M.S. Piekarczyk, L.L. Kiessling, A defined glycosaminoglycan-binding substratum for human pluripotent stem cells, Nat. Methods 7 (2010) 989–994.
[25] L.G. Villa-Diaz, H. Nandivada, J. Ding, N.C. Nogueira-de-Souza, P.H. Krebsbach, K.S. O'Shea, J. Lahann, G.D. Smith, Synthetic polymer coatings for long-term growth of human embryonic stem cells, Nat. Biotechnol. 28 (2010) 581–583.
[26] Z. Melkoumian, J.L. Weber, D.M. Weber, A.G. Fadeev, Y. Zhou, P. Dolley-Sonneville, J. Yang, L. Qiu, C.A. Priest, C. Shogbon, A.W. Martin, J. Nelson, P. West, J.P. Beltzer, S. Pal, R. Brandenberger, Synthetic peptide-acrylate surfaces for long-term self-renewal and cardiomyocyte differentiation of human embryonic stem cells, Nat. Biotechnol. 28 (2010) 606–610.
[27] E.F. Irwin, R. Gupta, D.C. Dashti, K.E. Healy, Engineered polymer-media interfaces for the long-term self-renewal of human embryonic stem cells, Biomaterials 32 (2011) 6912–6919.
[28] D.A. Brafman, C.W. Chang, A. Fernandez, K. Willert, S. Varghese, S. Chien, Long-term human pluripotent stem cell self-renewal on synthetic polymer surfaces, Biomaterials 31 (2010) 9135–9144.
[29] L. Liu, M. Yoshioka, M. Nakajima, A. Ogasawara, J. Liu, K. Hasegawa, S. Li, J. Zou, N. Nakatsuji, K.-i. Kamei, Y. Chen, Nanofibrous gelatin substrates for long-term expansion of human pluripotent stem cells, Biomaterials 35 (2014) 6259–6267.
[30] Y. Deng, X. Zhang, X. Zhao, Q. Li, Z. Ye, Z. Li, Y. Liu, Y. Zhou, H. Ma, G. Pan, D. Pei, J. Fang, S. Wei, Long-term self-renewal of human pluripotent stem cells on peptide-decorated poly(OEGMA-co-HEMA) brushes under fully defined conditions, Acta Biomater. 9 (2013) 8840–8850.
[31] H.J. Park, K. Yang, M.J. Kim, J. Jang, M. Lee, D.W. Kim, H. Lee, S.W. Cho, Bio-inspired oligovitronectin-grafted surface for enhanced self-renewal and long-term maintenance of human pluripotent stem cells under feeder-free conditions, Biomaterials 50 (2015) 127–139.
[32] K. Kandasamy, K. Narayanan, M. Ni, C. Du, A.C. Wan, D. Zink, Polysulfone membranes coated with polymerized 3,4-dihydroxy-l-phenylalanine are a versatile and cost-effective synthetic substrate for defined long-term cultures of human pluripotent stem cells, Biomacromolecules 15 (2014) 2067–2078.
[33] H. Li, D. Cui, H. Cai, L. Zhang, X. Chen, J. Sun, Y. Chao, Use of surface plasmon resonance to investigate lateral wall deposition kinetics and properties of polydopamine films, Biosens. Bioelectron. 41 (2013) 809–814.
[34] H. Lee, S.M. Dellatore, W.M. Miller, P.B. Messersmith, Mussel-inspired surface chemistry for multifunctional coatings, Science 318 (2007) 426–430.
[35] S. Jin, H. Yao, J.L. Weber, Z.K. Melkoumian, K. Ye, A synthetic, xeno-free peptide surface for expansion and directed differentiation of human induced pluripotent stem cells, PLoS One 7 (2012) e50880.
[36] H. Lee, J. Rho, P.B. Messersmith, Facile conjugation of biomolecules onto surfaces via mussel adhesive protein inspired coatings, Adv. Mater. 21 (2009) 431–434.
[37] K. Yang, J.S. Lee, J. Kim, Y.B. Lee, H. Shin, S.H. Um, J.B. Kim, K.I. Park, H. Lee, S.W. Cho, Polydopamine-mediated surface modification of scaffold materials for human neural stem cell engineering, Biomaterials 33 (2012) 6952–6964.
[38] W.C. Low, P.O. Rujitanaroj, D.K. Lee, P.B. Messersmith, L.W. Stanton, E. Goh, S.Y. Chew, Nanofibrous scaffold-mediated REST knockdown to enhance neuronal differentiation of stem cells, Biomaterials 34 (2013) 3581–3590.
[39] Y.J. Lee, J.H. Lee, H.J. Cho, H.K. Kim, T.R. Yoon, H. Shin, Electrospun fibers immobilized with bone forming peptide-1 derived from BMP7 for guided bone regeneration, Biomaterials 34 (2013) 5059–5069.
[40] G. Chen, Y. Xia, X. Lu, X. Zhou, F. Zhang, N. Gu, Effects of surface functionalization of PLGA membranes for guided bone regeneration on proliferation and behavior of osteoblasts, J. Biomed. Mater. Res. A 101A (2013) 44–53.
[41] N.G. Rim, S.J. Kim, Y.M. Shin, I. Jun, D.W. Lim, J.H. Park, H. Shin, Mussel-inspired surface modification of poly(L-lactide) electrospun fibers for modulation of osteogenic differentiation of human mesenchymal stem cells, Coll. Surf. B. Biointerfaces 91 (2012) 189–197.
[42] M. Lai, K. Cai, L. Zhao, X. Chen, Y. Hou, Z. Yang, Surface Functionalization of TiO_2 nanotubes with bone morphogenetic protein 2 and its synergistic effect on the differentiation of mesenchymal stem cells, Biomacromolecules 12 (2011) 1097–1105.
[43] Y.M. Shin, H. Park, H. Shin, Enhancement of cardiac myoblast responses onto electrospun PLCL fibrous matrices coated with polydopamine for gelatin immobilization, Macromol. Res. 19 (2011) 835–842.
[44] J. Park, T.F. Brust, H.J. Lee, S.C. Lee, V.J. Watts, Y. Yeo, Polydopamine-based simple and versatile surface modification of polymeric nano drug carriers, ACS Nano 8 (2014) 3347–3356.
[45] J. Cui, Y. Yan, G.K. Such, K. Liang, C.J. Ochs, A. Postma, F. Caruso, Immobilization and intracellular delivery of an anticancer drug using mussel-inspired polydopamine capsules, Biomacromolecules 13 (2012) 2225–2228.
[46] S.H. Hwang, D. Kang, R.S. Ruoff, H.S. Shin, Y.-B. Park, Poly(vinyl alcohol) reinforced and toughened with poly(dopamine)-treated graphene oxide, and its use for humidity sensing, ACS Nano 8 (2014) 6739–6747.
[47] H.P. Peng, R.P. Liang, L. Zhang, J.D. Qiu, Facile preparation of novel core–shell enzyme–Au–polydopamine–Fe_3O_4 magnetic bionanoparticles for glucose-sensor, Biosens. Bioelectron. 42 (2013) 293–299.
[48] W.F. Zhang, X.T. Zhao, Q.S. Zhao, S.H. Zha, D.M. Liu, Z.J. Zheng, W.T. Li, H.Y. Zhou, Y. Yan, Biocompatibility and characteristics of theophylline/carboxymethyl chitosan microspheres for pulmonary drug delivery, Polym. Int. 63 (2014) 1035–1040.
[49] S.Y. Huang, B.Q. Han, K. Shao, M. Yu, W.S. Liu, Analgesic and wound healing effect of chitosan and carboxymethyl chitosan on scalded rats, J. Ocean Univ. China 13 (2014) 837–841.
[50] L. Wang, L. Wang, W. Huang, H. Su, Y. Xue, Z. Su, B. Liao, H. Wang, X. Bao, D. Qin, J. He, W. Wu, K.F. So, G. Pan, D. Pei, Generation of integration-free neural progenitor cells from cells in human urine, Nat. Methods 10 (2013) 84–89.
[51] B.E. Reubinoff, M.F. Pera, G. Vajta, A.O. Trounson, Effective cryopreservation of human embryonic stem cells by the open pulled straw vitrification method, Hum. Reprod. 16 (2001) 2187–2194.
[52] Y. Zhou, P. Zhou, Y. Xin, J. Wang, Z. Zhu, J. Hu, S. Wei, H. Ma, Trend of telomerase activity change during human iPSC self-renewal and differentiation revealed by a quartz crystal microbalance based assay, Sci. Rep. 4 (2014) 6978.
[53] P.W. Burridge, E. Matsa, P. Shukla, Z.C. Lin, J.M. Churko, A.D. Ebert, F. Lan, S. Diecke, B. Huber, N.M. Mordwinkin, J.R. Plews, O.J. Abilez, B.X. Cui, J.D. Gold, J.C. Wu, Chemically defined generation of human cardiomyocytes, Nat. Methods 11 (2014) 855–860.
[54] R. Wang, K.G. Neoh, Z. Shi, E.T. Kang, P.A. Tambyah, E. Chiong, Inhibition of *Escherichia coli* and *Proteus mirabilis* adhesion and biofilm formation on medical grade silicone surface, Biotechnol. Bioeng. 109 (2012) 336–345.
[55] S.L. Bellis, Advantages of RGD peptides for directing cell association with biomaterials, Biomaterials 32 (2011) 4205–4210.
[56] W. Chen, L.G. Villa-Diaz, Y. Sun, S. Weng, J.K. Kim, R.H.W. Lam, L. Han, R. Fan, P.H. Krebsbach, J. Fu, Nanotopography influences adhesion, spreading, and self-renewal of human embryonic stem cells, ACS Nano 6 (2012) 4094–4103.
[57] F. Chowdhury, Y. Li, Y.-C. Poh, T. Yokohama-Tamaki, N. Wang, T.S. Tanaka, Soft wubstrates promote homogeneous self-renewal of embryonic stem cells via downregulating cell-matrix tractions, PLoS One 5 (2010) e15655.
[58] L. Upadhyaya, J. Singh, V. Agarwal, R.P. Tewari, The implications of recent advances in carboxymethyl chitosan based targeted drug delivery and tissue engineering applications, J. Control Release 186 (2014) 54–87.
[59] J. Beers, D.R. Gulbranson, N. George, L.I. Siniscalchi, J. Jones, J.A. Thomson, G. Chen, Passaging and colony expansion of human pluripotent stem cells by enzyme-free dissociation in chemically defined culture conditions, Nat. Protoc. 7 (2012) 2029–2040.
[60] K. Watanabe, M. Ueno, D. Kamiya, A. Nishiyama, M. Matsumura, T. Wataya, J.B. Takahashi, S. Nishikawa, S.I. Nishikawa, K. Muguruma, Y. Sasai, A ROCK inhibitor permits survival of dissociated human embryonic stem cells, Nat. Biotechnol. 25 (2007) 681–686.
[61] B. Choi, K.S. Park, J.H. Kim, K.W. Ko, J.S. Kim, D.K. Han, S.H. Lee, Stiffness of hydrogels regulates cellular reprogramming efficiency through mesenchymal-to-epithelial transition and stemness markers, Macromol. Biosci. (2015), http://dx.doi.org/10.1002/mabi.201500273.
[62] N. Heins, M.C.O. Englund, C. Sjöblom, U. Dahl, A. Tonning, C. Bergh, A. Lindahl, C. Hanson, H. Semb, Derivation, characterization, and differentiation of human embryonic stem cells, Stem Cells 22 (2004) 367–376.
[63] J. Zhou, A.V. Ellis, N.H. Voelcker, Recent developments in PDMS surface modification for microfluidic devices, Electrophoresis 31 (2010) 2–16.
[64] J. Zhou, D.A. Khodakov, A.V. Ellis, N.H. Voelcker, Surface modification for PDMS-based microfluidic devices, Electrophoresis 33 (2012) 89–104.